

Supporting Information

Observing Long-lived Photogenerated Holes in Cobalt Oxyhydroxide Oxygen Evolution Catalysts

Ruben Mirzoyan, Alec H. Follmer, and Ryan G. Hadt*

Division of Chemistry and Chemical Engineering, Arthur Amos Noyes Laboratory of Chemical Physics, California Institute of Technology, Pasadena, California 91125, United States

*Corresponding author: rghadt@caltech.edu

Table of Contents

Materials and Methods.....	2
Materials.....	2
Electrochemical Methods.....	2
Film Preparation.....	2
Measuring Double Layer Capacitance.....	3
Steady State UV-Vis Absorption and Spectroelectrochemistry.....	3
Ultrafast Transient Absorption (TA) and TA Spectroelectrochemistry.....	3
Nanosecond/ Microsecond/ Millisecond TA.....	3
Profilometry.....	4
Fitting of Kinetic Traces.....	4
Figures.....	5
Tables.....	31
References.....	36

Materials and Methods

Materials. $\text{Co}(\text{NO}_3)_2$ 99.999%, K_2HPO_4 99.99%, H_3BO_3 99.999%, KOH 99.99% were used as received from Millipore Sigma. All electrolyte solutions were prepared with MilliPore filtered water with 18.20 $\text{M}\Omega\text{-cm}$ resistivity. All experiments used fluorine-tin-oxide (FTO; TEC-7) coated glass slides that were purchased as pre-cut 1 cm \times 2.5 cm glass piece from MSE Supplies.

Electrochemical Methods. Aqueous electrochemical measurements were conducted using a BioLogic VSP-300 Potentiostat, a Ag/AgCl reference electrode with saturated KCl from BASi and a high surface area Pt-mesh counter electrode. Aqueous experiments were performed using a three-electrode electrochemical cell consisting of 25 mL of electrolyte solution. Experiments were performed at ambient temperature (21 °C) and electrode potentials were converted to the NHE scale using $E(\text{NHE}) = E(\text{Ag}/\text{AgCl}) + 0.199 \text{ V}$. Phosphate (Pi) buffers were made to contain 0.1 M phosphate and were adjusted to pH 7.00. Borate (Bi) buffers were made to contain 0.1 M borate and were adjusted to pH 9.20. Non-aqueous electrochemical measurements were conducted in 0.1 M TBAPF₆ in acetonitrile. A non-aqueous reference electrode containing a silver wire and a CoralPor® tip from BASi was used and filled with 0.010 M AgPF₆ (Millipore Sigma) and 0.1 M TBAPF₆ (Millipore Sigma) acetonitrile solution. Pt-mesh was used as the counter electrode. Acetonitrile was dried prior to use, however, the experiments were conducted in ambient conditions and trace amounts of water are expected to be present. Cyclic voltammograms and absorbance spectra from water titration experiments were done by starting from acetonitrile, rinsing, cleaning, and drying the electrochemical cell container (a 1.0 cm pathlength cuvette), and filling with a prepared acetonitrile solution of known aqueous buffer content (1%, 2% and 5%). Phosphate buffer was used for CoPi, while borate buffer was used for CoBi.

Film Preparation. Catalyst films of CoPi (CoBi) were prepared via chronoamperometry of Pi (Bi) electrolyte solutions containing 0.5 mM $\text{Co}(\text{NO}_3)_2$. FTO-coated glass pieces were used as the working and electrode and rinsed with acetone and water prior to use. A piece of Scotch tape was affixed to the electrode such that 1.0 cm² area was exposed to the electrolyte solution. At a potential of 1.05 V vs. NHE, chronoamperometry is carried out and the charge passed in mC/cm² is used as a proxy for the thickness of the catalyst film. A typical steady-state deposition current density is 6

mA·h/s. CoPi and CoBi film preparation methods were consistent with methods established in the literature.¹⁻³

Measuring Double Layer Capacitance. Metrics proportional to the electrochemically active surface area (ECSA) were acquired based on an established procedure,⁴ with results presented in **Figure S33**. A non-Faradaic region of the CV was chosen for the scanning range and the double layer capacitance was determined from the slope when fitting the non-faradaic current difference at the end points to the scan rate.

Steady State UV-Vis Absorption and Spectroelectrochemistry. Absorption spectra were recorded with a StellarNet BLACK-Comet UV-VIS Spectrometer, with two separate light sources (SL1 Tungsten Halogen Lamp and SL3 UV Deuterium Source). The FTO-coated glass pieces with deposited catalyst were placed vertically in a 1.0 cm pathlength quartz cuvette with the catalyst-coated side in contact with the corresponding native Co²⁺-free buffer. The potentiostat was connected to the electrodes in the cuvette and spectra were recorded after 60 seconds of exposure to each applied potential. Heating of the sample was achieved by a Unisoku USP-203 cryostat sample holder.

Ultrafast Transient Absorption (TA) and TA Spectroelectrochemistry. The 800 nm output of a 5 W, 1 kHz pulsed Ti:sapphire amplifier (Coherent Astrella) was split with a 50:50 beamsplitter. One half was fed into an OPerA Solo optical parametric amplifier tuned to a 380 nm output, which was used as the excitation pump and routed through a femtosecond HELIOS FIRE transient absorption spectrometer (Ultrafast Systems). The other half was used to generate broadband probe light of the visible wavelength region. The resulting pulse-width at the sample was 120 fs, as measured from fitting of the instrument response function on various samples. Samples were measured in a 1.0 cm pathlength quartz cuvette in their native Co²⁺-free buffers. In the case of applied anodic bias, the 1.0 cm cuvette served as a three-electrode cell. Transient absorption spectra were collected as the sample was held at various externally applied potentials.

Nanosecond/ Microsecond/ Millisecond TA. A tunable 10 Hz OPOTEK laser was used to generate a pump pulse of 10 ns pulse-width, while a Xenon arc lamp was used to generate the probe light. A monochromator set to isolate a specific probe wavelength was used. A

photomultiplier tube with 10^4 V/A gain was used and the signal was digitized (with full bandwidth in the case of ≤ 100 μ s time range, and 1 MHz bandwidth in the case of 10 MHz time range) to generate the resulting ΔA signal.

Profilometry. Profilometry measurements were taken with a DektakXT Stylus Profilometer with a 2 μ m stylus tip diameter. Software leveling was implemented with the “Terms Removal (F-Operator)” method.⁵ Multiple measurements were made at varying lateral cross-sections for each film, and the average thickness and standard deviation was computed by scanning from the FTO surface to the cobalt oxide film over the span of a few mm and taking the data where the height of the film levels off after the initial height step (which tended to have remnants of adhesive and seeming more film deposition near the edge).

Fitting of Kinetic Traces. All ultrafast (1000 Hz) spectral cuts shown were chirp corrected to a 3rd order polynomial and time-zero corrected.

To fit the excited state decays as collected from the 10 Hz laser up to time delays of 10 ms, several trial functions were tested. The initial maximum intensity value of the data was taken as time zero. The trial functions comprised of the following:

“Biexponential”:

$$\Delta OD = a_1 \exp(-k_1 t) + a_2 \exp(-k_2 t)$$

“Triexponential”:

$$\Delta OD = a_1 \exp(-k_1 t) + a_2 \exp(-k_2 t) + a_3 \exp(-k_3 t)$$

“Two exponentials, one stretched exponential”:

$$\Delta OD = a_1 \exp(-k_1 t) + a_2 \exp(-k_2 t) + a_3 \exp((-k_3 t)^\beta)$$

“Two stretched exponentials”:

$$\Delta OD = a_1 \exp((-k_1 t)^\beta) + a_2 \exp((-k_2 t)^\beta)$$

A non-linear least squares method was used with a function tolerance of $1e-7$, optimality tolerance of $1e-7$, step tolerance of $1e-7$, maximum iterations of $1e-4$ and maximum function evaluations of $5e3$. These fits are implicated and detailed in **Figures S34-S36** and **Tables S2-S4**.

Figures

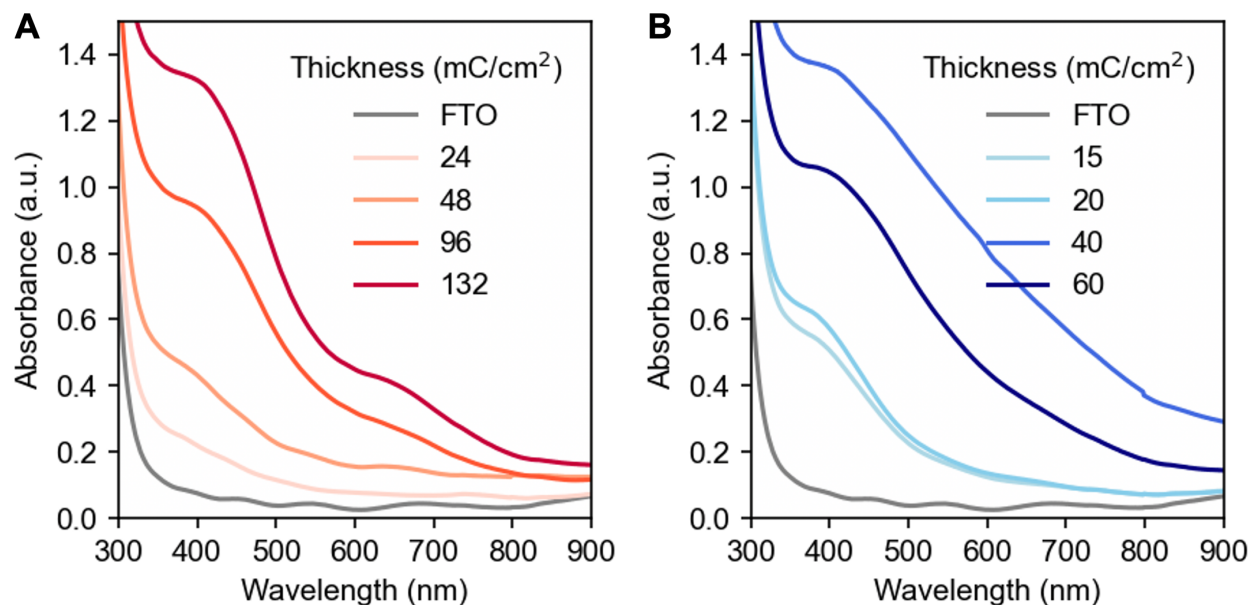


Figure S1: Absorption spectra of CoPi (A) and CoBi (B) films of various thicknesses in their native buffers. The reference spectrum was a piece of FTO immersed in the native buffer without any deposited material. Thin film interference results in oscillations in the frequency domain superimposed on the absorptive features.

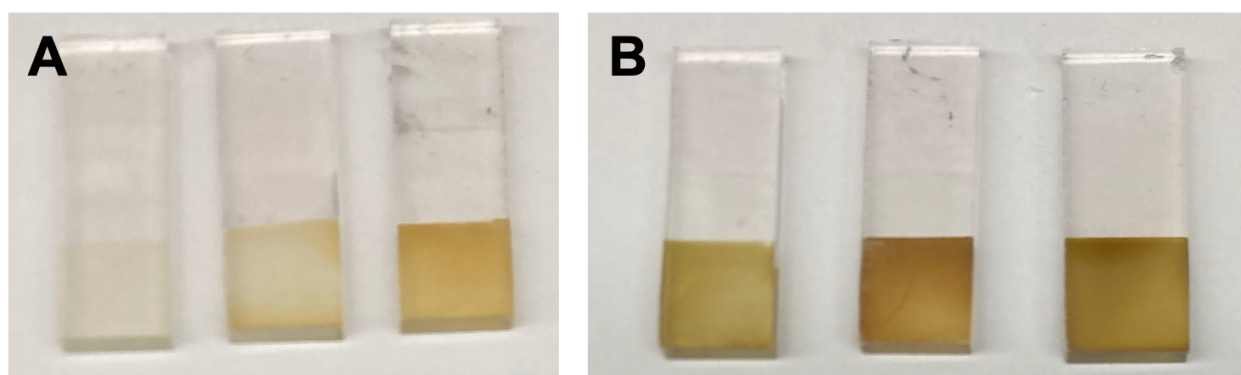


Figure S2. A) CoBi films of 10 mC/cm², 20 mC/cm² and 40 mC/cm² thickness. B) CoPi films of 24 mC/cm², 48 mC/cm² and 96 mC/cm² thickness.

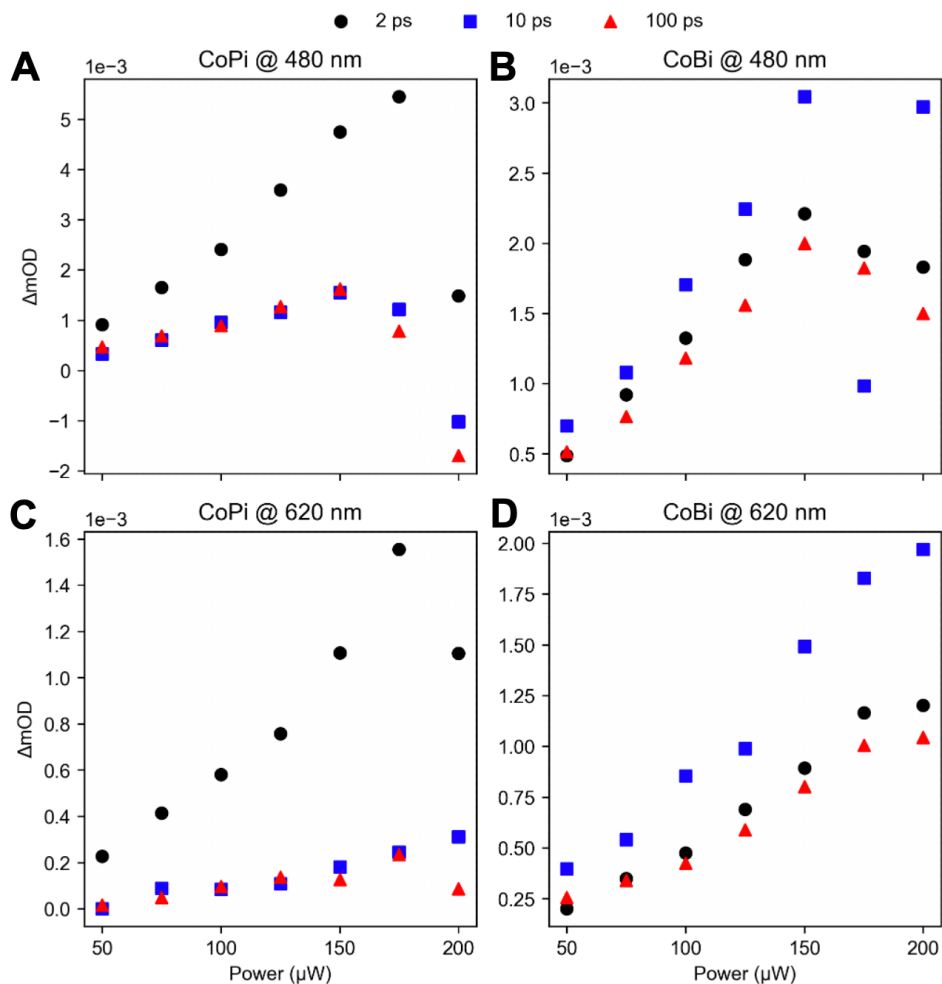


Figure S3. Power dependence of ultrafast 120 fs pulse-width 380 nm pump TA signal for 48 mC/cm^2 CoPi (A, C) and 20 mC/cm^2 CoBi (B, D). A pump power of 100 μW was used for all transient absorption studies as it is well within the linear regime.

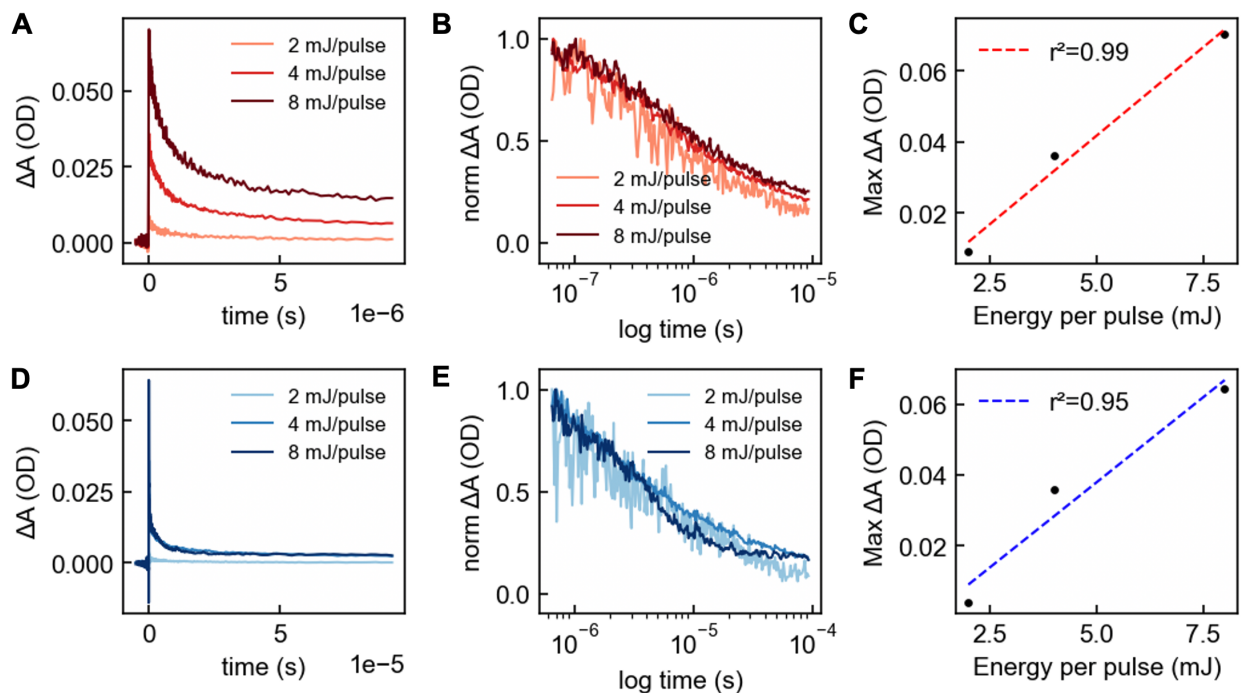


Figure S4. Power dependence of 380 nm pump with 10 ns pulse-width laser transient absorption signal for CoPi (A, B, C) and CoBi (D, E, F) immersed in H₂O. Pulse energies below 8 mJ/pulse were used for all experiments. The spot size diameter is on the order of 1 cm.

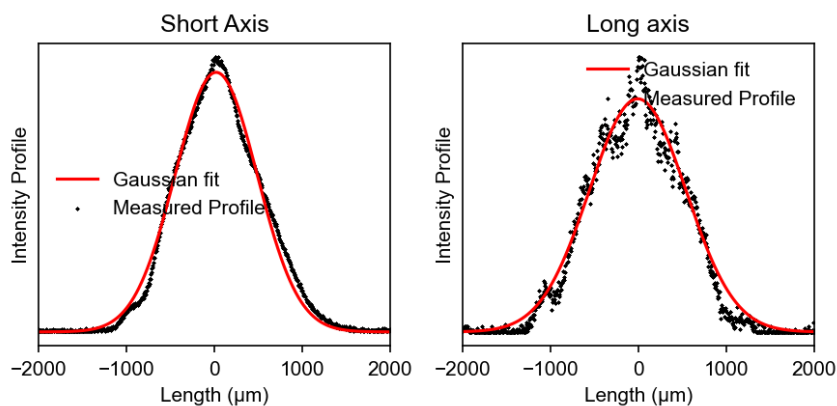


Figure S5. Intensity profiles of the 380 nm ultrafast pump beam at the sample position (FWHM: 1100 μm for short axis, 1200 μm for long axis).

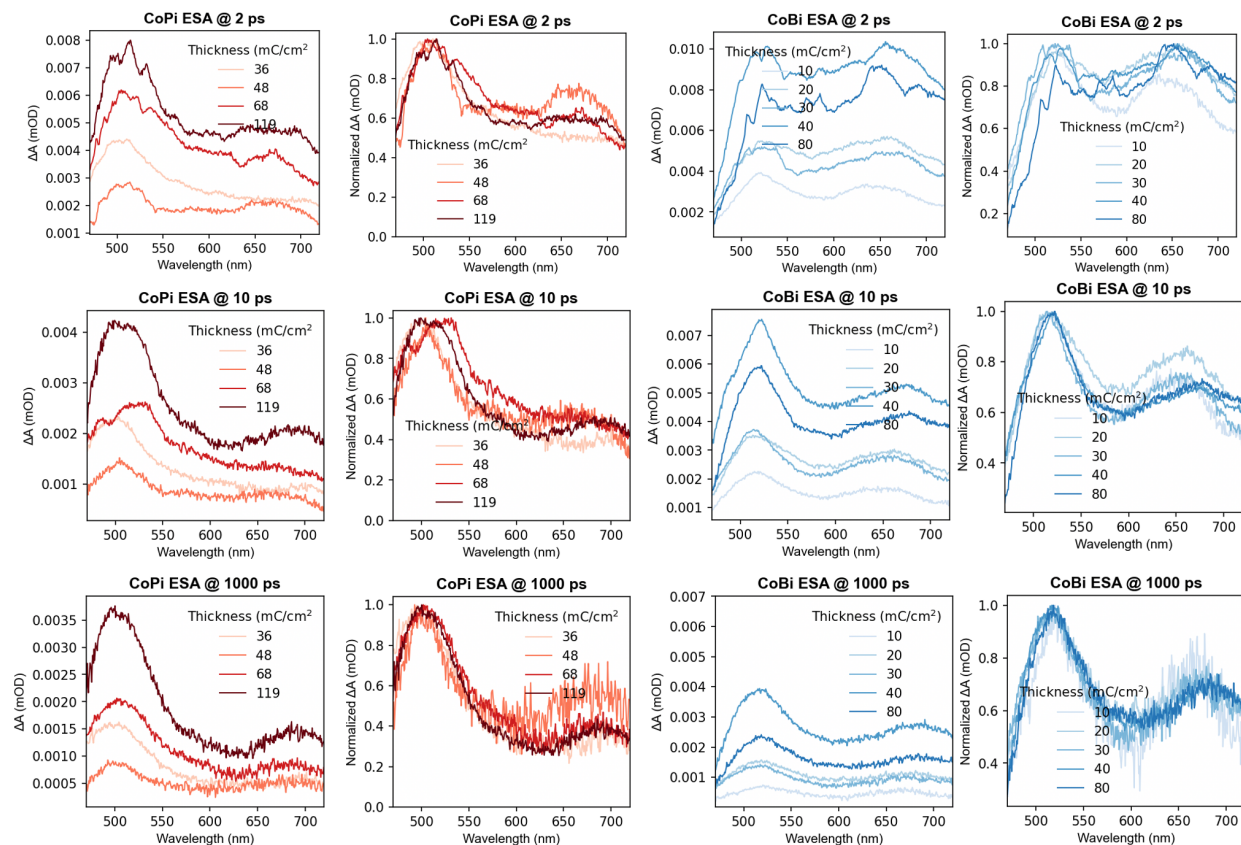


Figure S6. Thickness dependence of transient absorption spectral traces of CoPi and CoBi films at characteristic time delays. Overlaid normalized spectra are shown next to the unnormalized spectra.

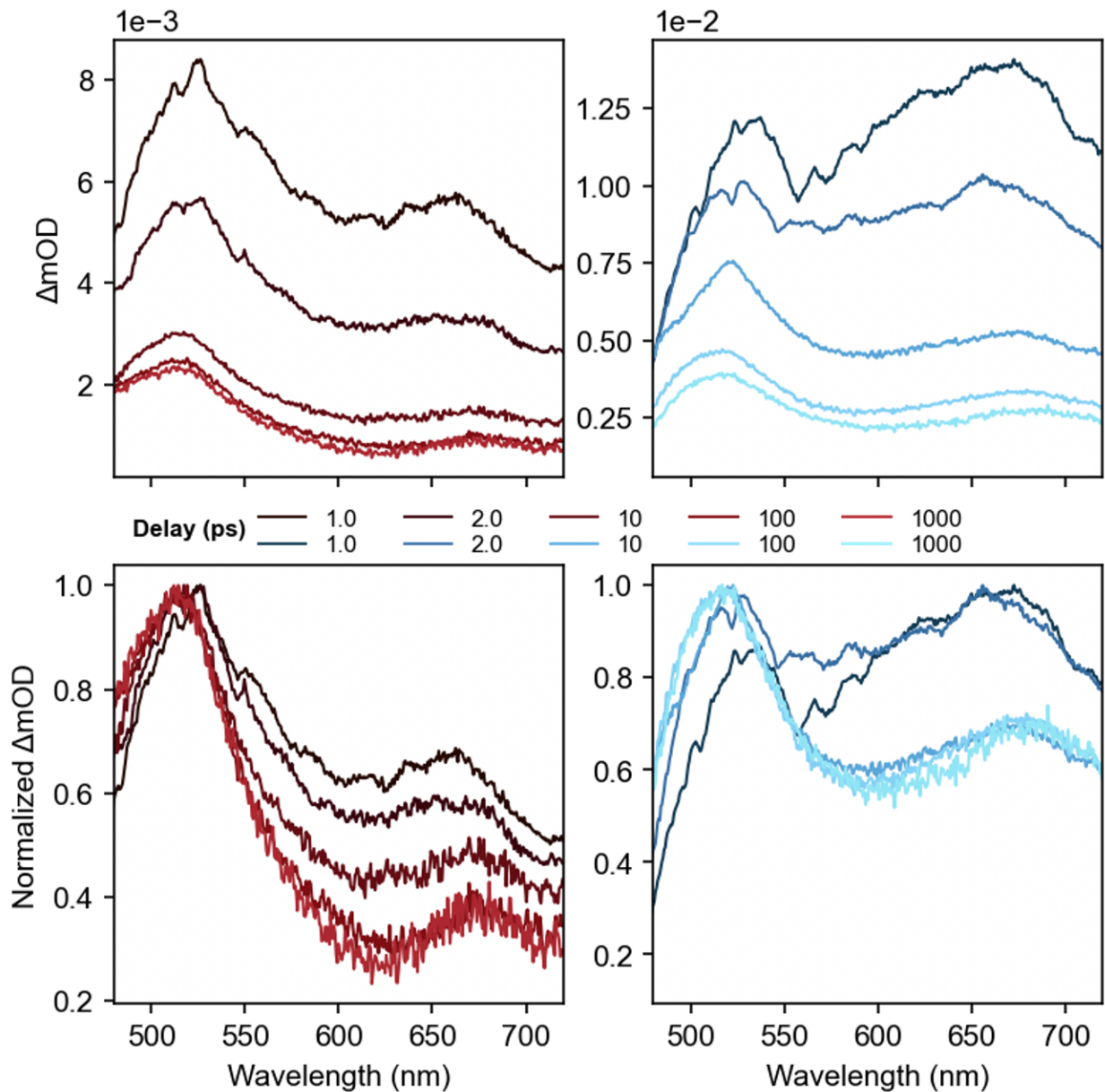


Figure S7. Transient absorption spectral traces at time delays of 2 ps, 10 ps and 1000 ps with applied bias of 96 mC/cm² CoPi (**A**, **C**, **E**) and 48 mC/cm² CoBi (**B**, **D**, **F**) films in their respective native buffers. Samples were pumped at 380 nm with a 120 fs pulse-width ultrafast laser.

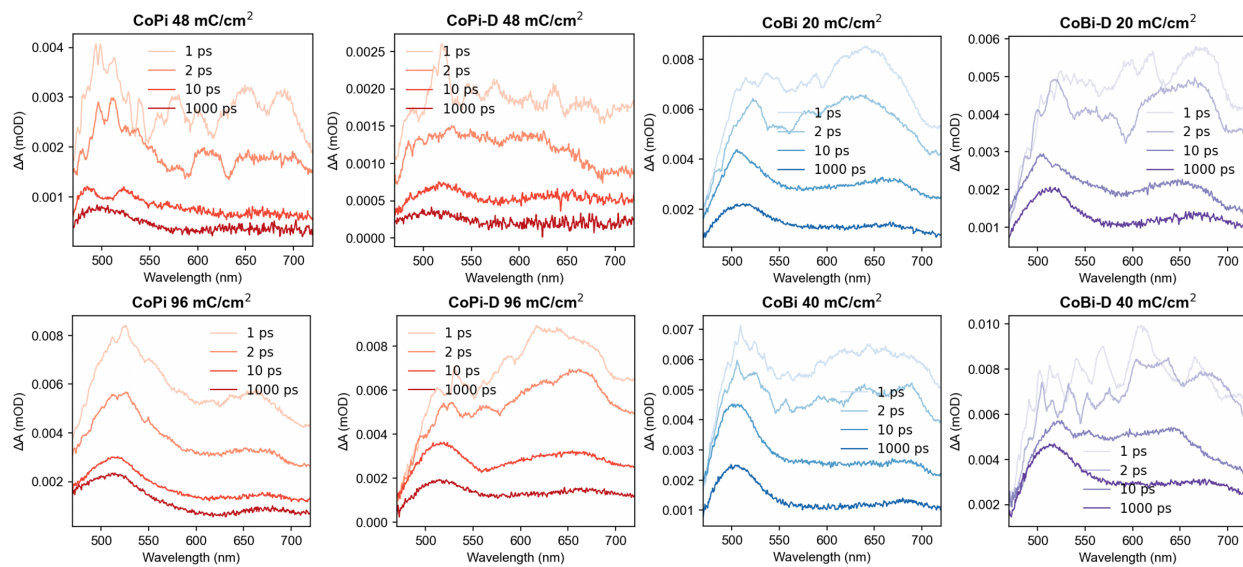


Figure S8. Transient absorption spectral traces for CoPi and CoBi in their respective buffers, both deuterated and non-deuterated. Samples were pumped at 380 nm with a 120 fs pulse-width ultrafast laser.

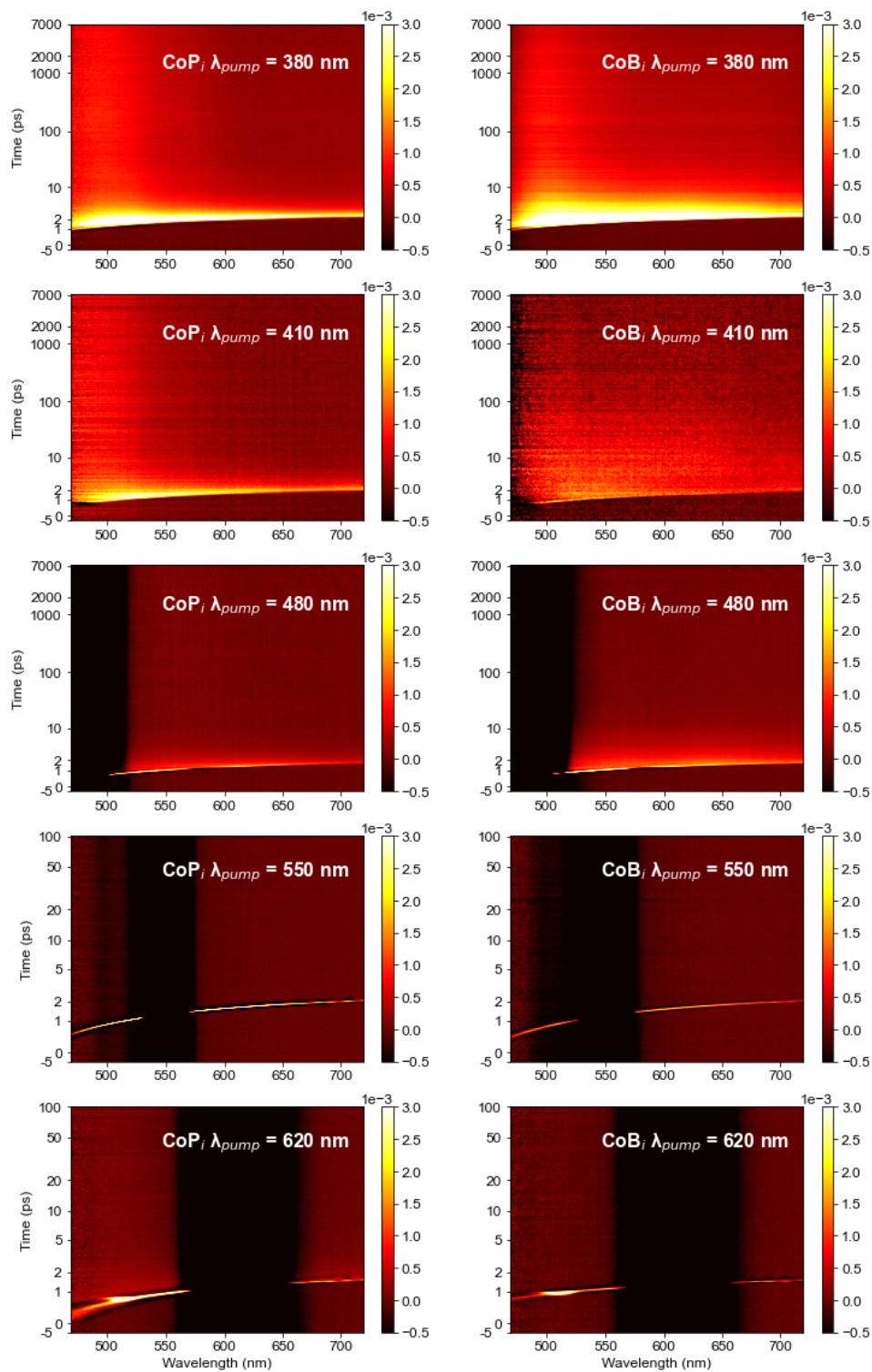


Figure S9. Pump wavelength dependence of ultrafast transient absorption spectra of films taken in their respective buffer solutions with 120 fs pulse-width ultrafast laser.

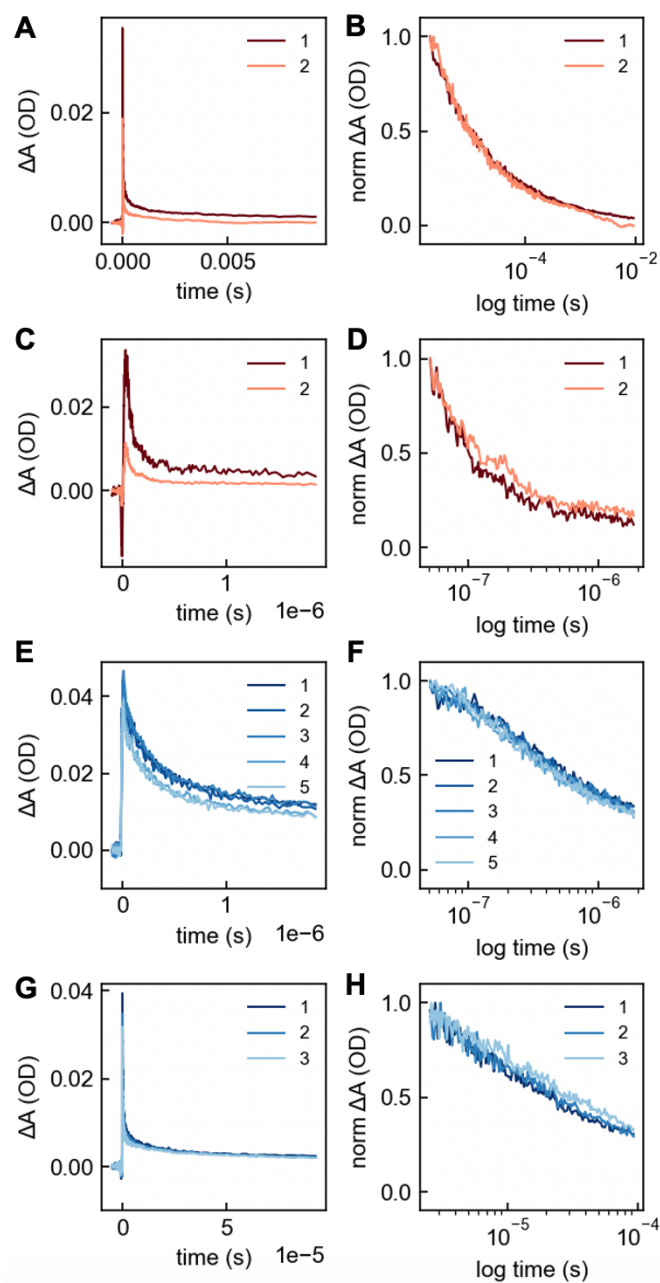


Figure S10. Successive shots of 380 nm pump of 10 ns pulse-width laser showing film dissolution effects for CoPi (A, B, C, D) and CoBi (E, F, G, H) in H₂O.

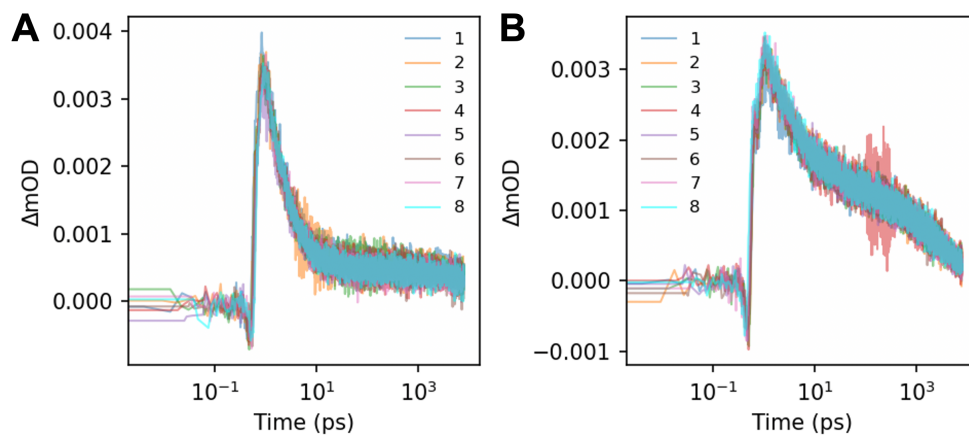


Figure S11. Successive ultrafast TA scans at a pump wavelength of 380 nm and 0.1 μJ pulse energy with a 10 ns pulse-width laser, suggesting no film dissolution or decomposition upon continued irradiation at the corresponding fluence.

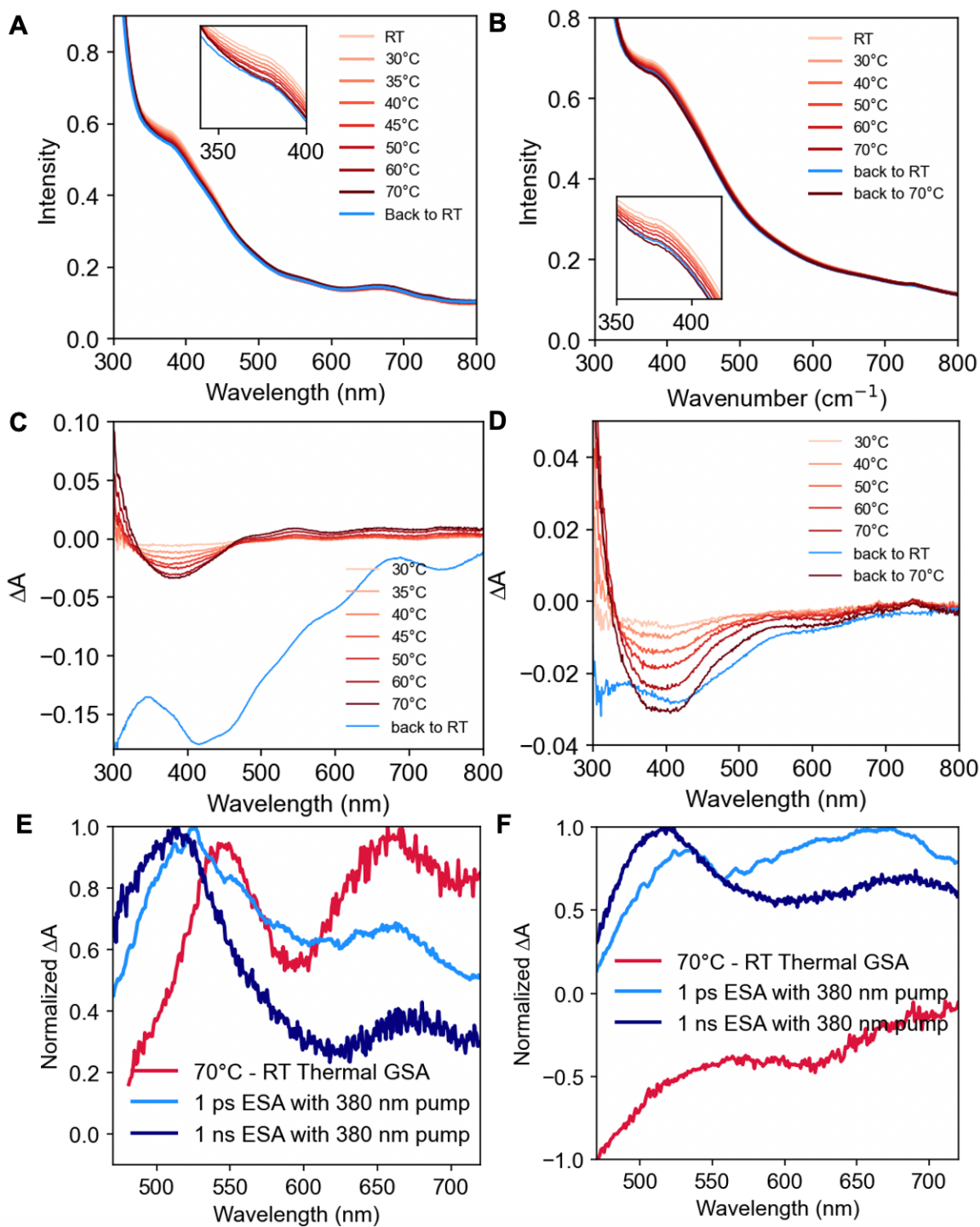


Figure S12. Effects of increased temperature on the absorption spectra of CoPi (A) and CoBi (B) films, with respective difference spectra (C, D) taken in their respective buffer solutions. Comparisons between the thermal difference spectra and excited state absorption spectra at representative time delays of 1 ps and 1 ns are shown for CoPi (E) and CoBi (F).

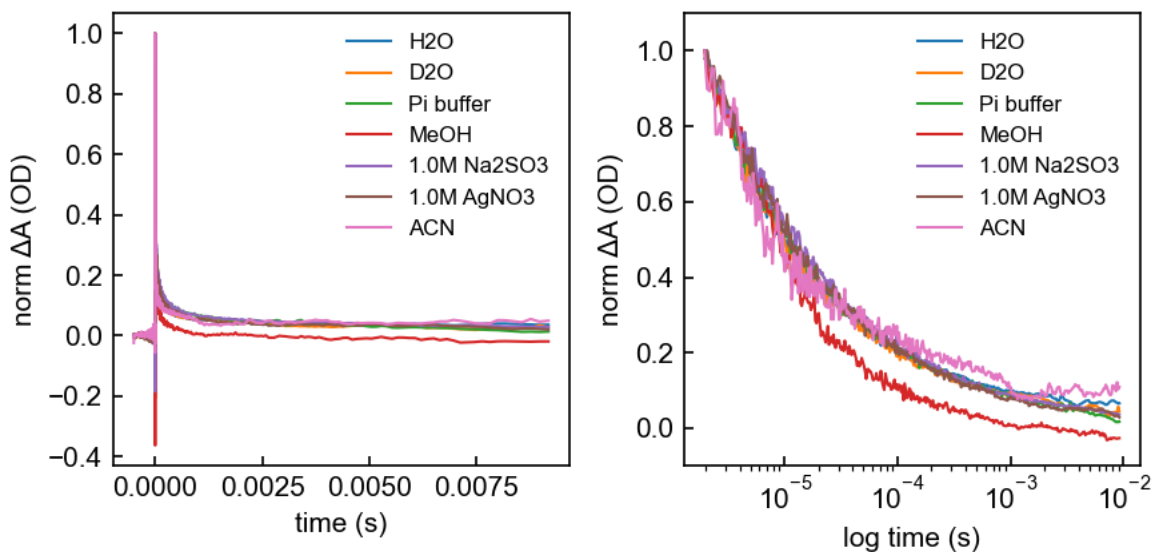


Figure S13. A comparison of 10 ms time range decays of a CoPi film in various media. The sample was translated between measurements in different solvents, such that the pump and probe were hitting a new non-photodegraded spot on the film for each measurement. A quenching effect is observed with MeOH.

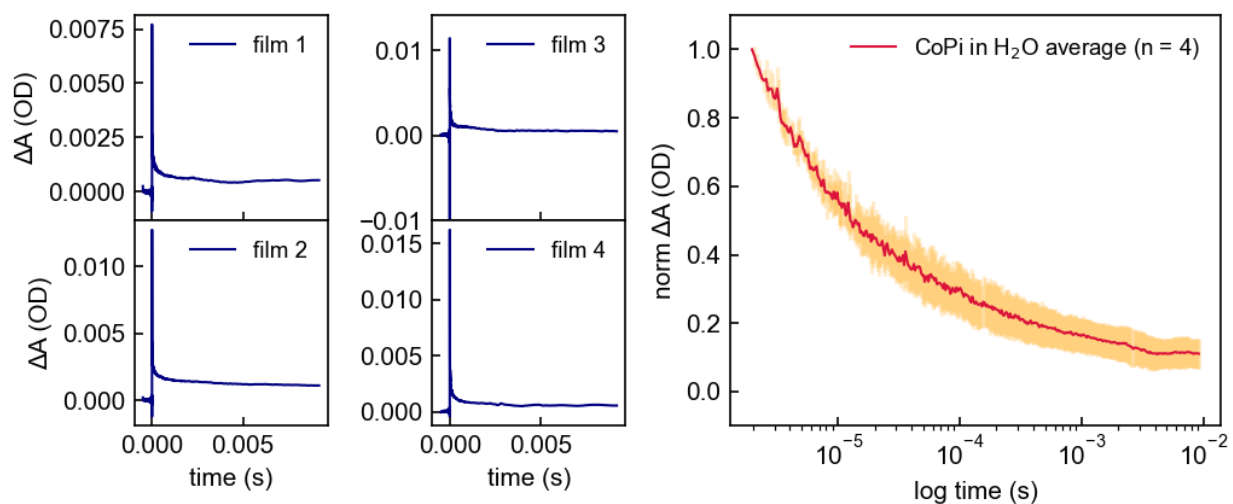


Figure S14. 10 ms time range decays of various CoPi films in H₂O, with average decay curve displayed.

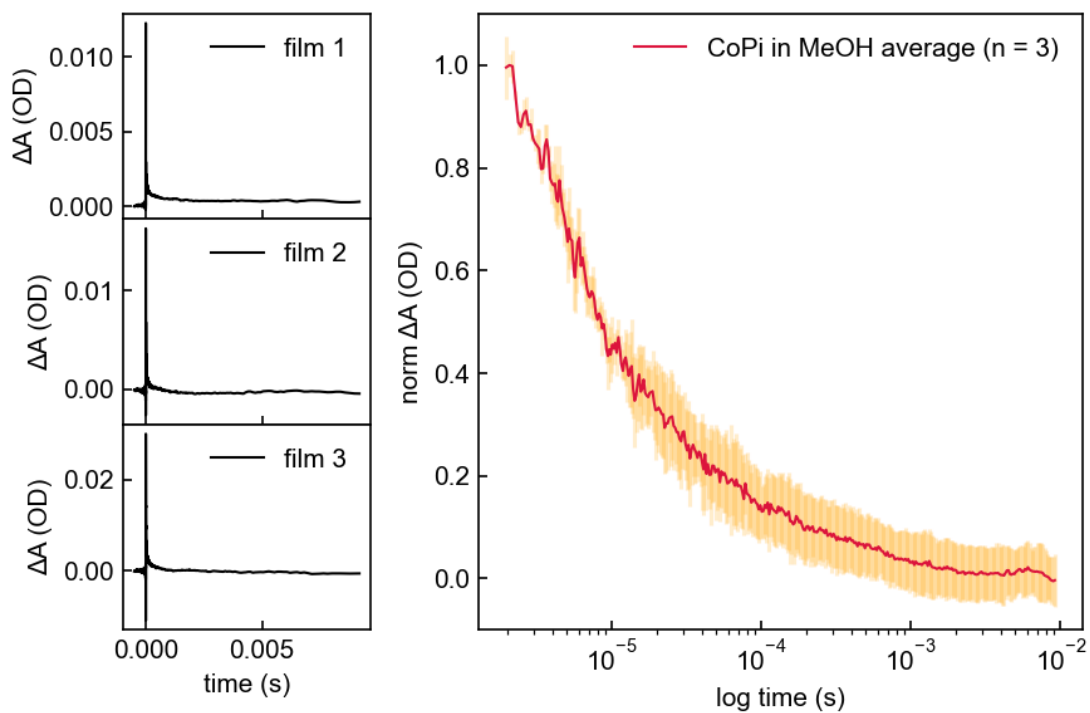


Figure S15. 10 ms time range decays of various CoPi films in MeOH, with average decay curve displayed.

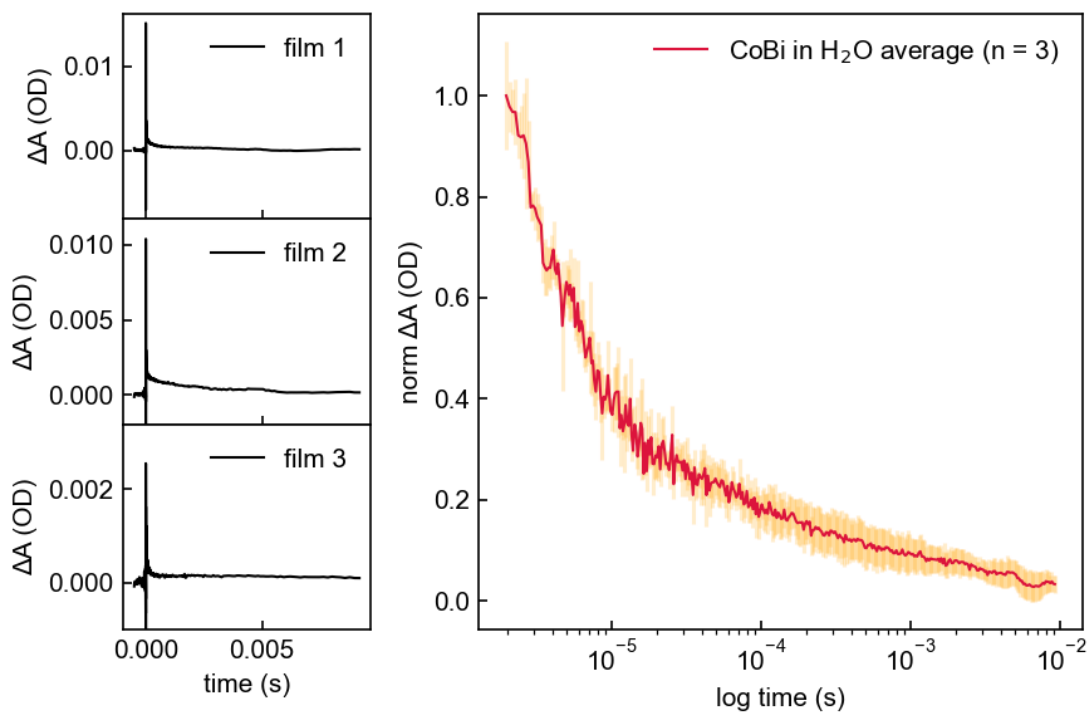


Figure S16. 10 ms time range decays of various CoBi films in H₂O, with average decay curve displayed.

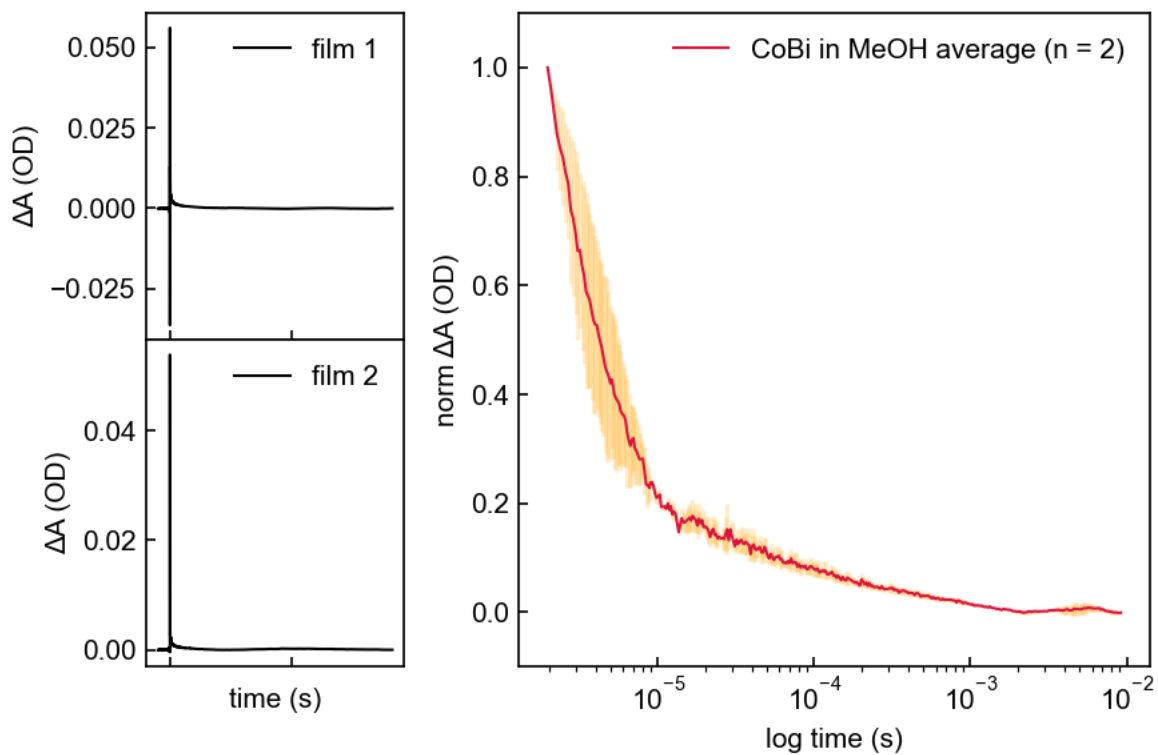


Figure S17. 10 ms time range decays of various CoBi films in MeOH, with average decay curve displayed.

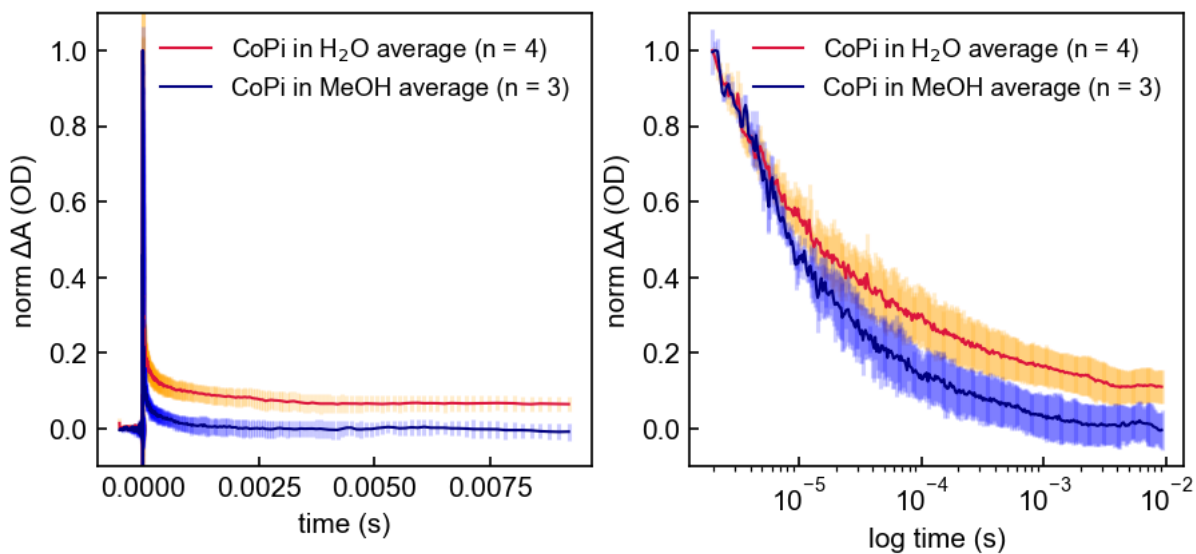


Figure S18. A comparison of average 10 ms time range decays of CoPi films in H₂O compared to CoPi films in MeOH.

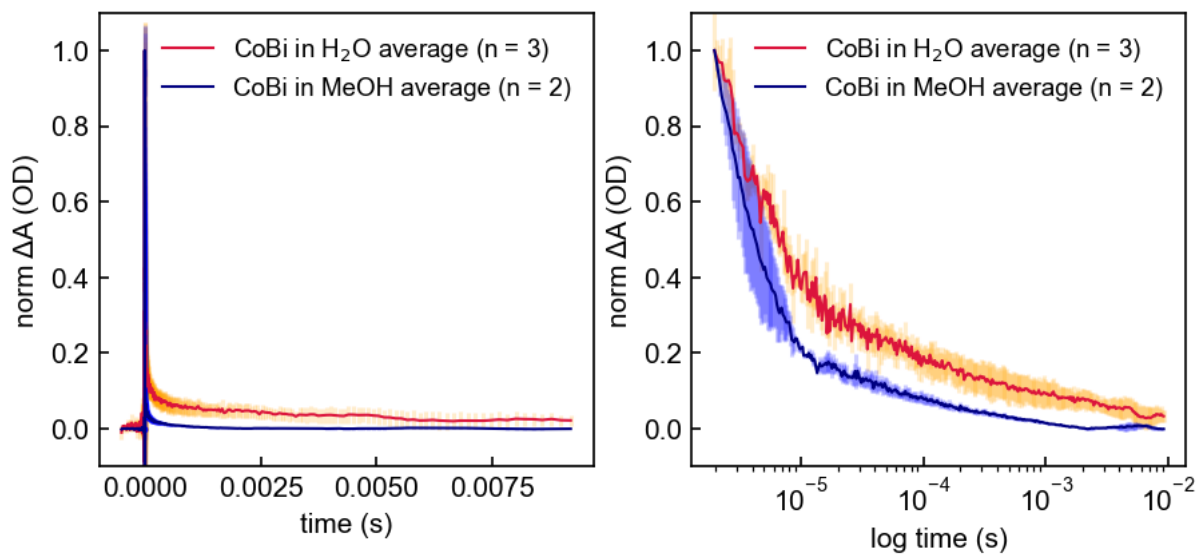


Figure S19. A comparison of average 10 ms time range decays of CoBi films in H₂O compared to CoBi films in MeOH.

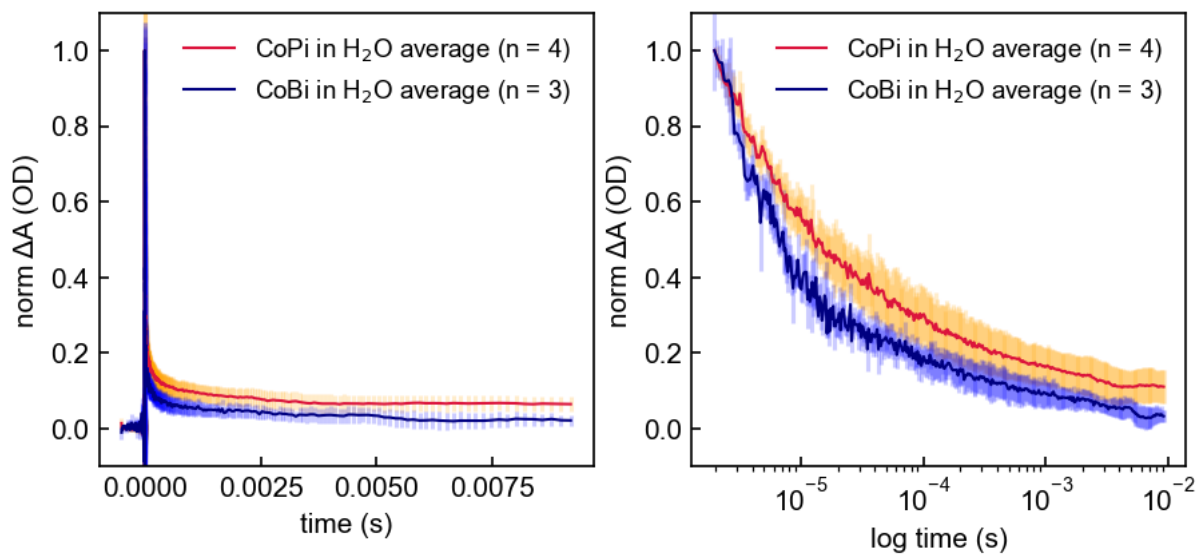


Figure S20. A comparison of average 10 ms time range decays of CoPi films in H₂O compared to CoBi films in H₂O.

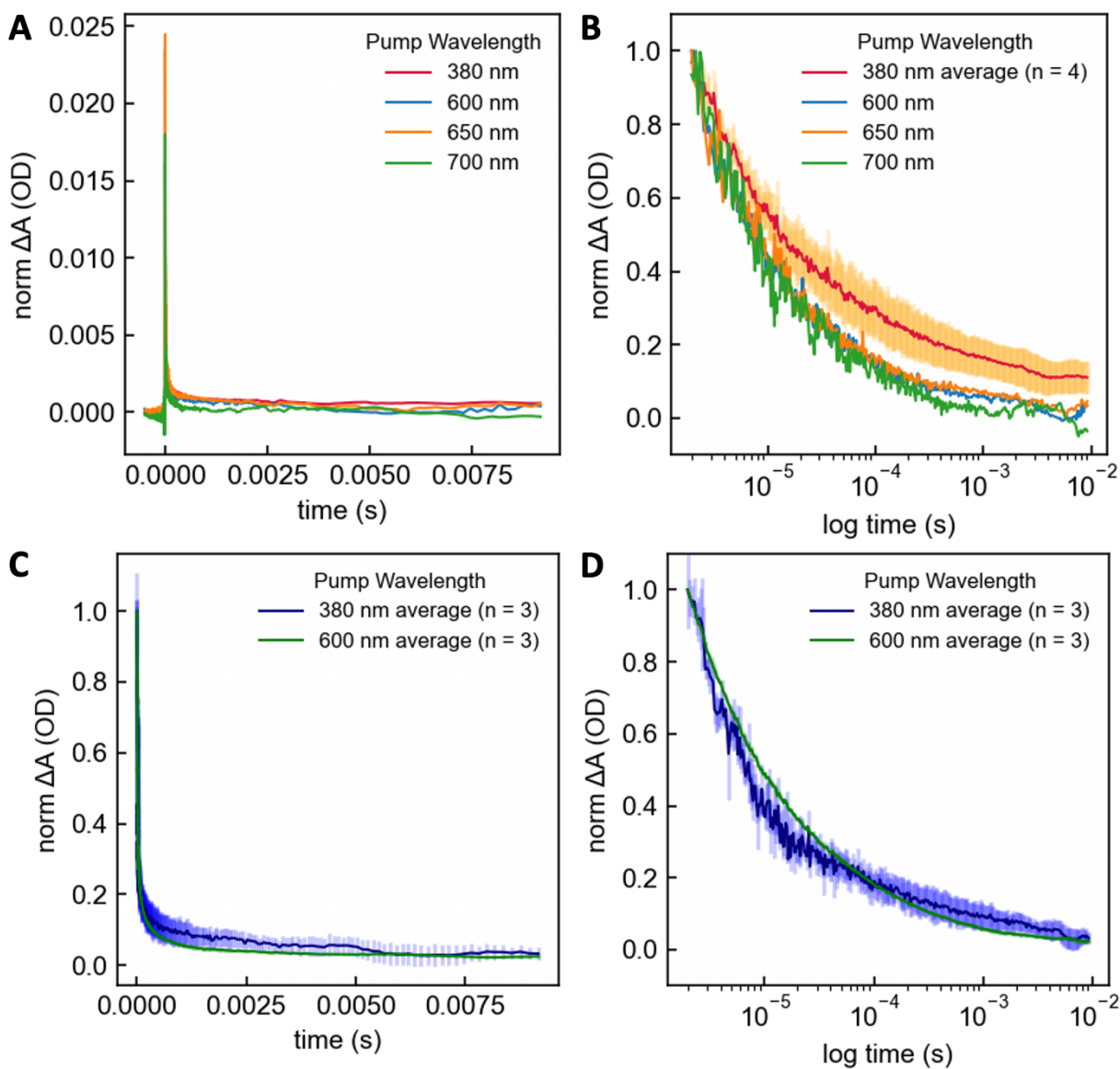


Figure S21. Pump wavelength dependent decay traces taken with 10 ns pulse-width laser probed at 500 nm. CoPi 4 mJ/pulse traces at varying pump wavelengths on a linear (A) and logarithmic (B) time scale. CoBi 4mJ/pulse traces at varying pump wavelengths on a linear (C) and logarithmic (D) time scale.

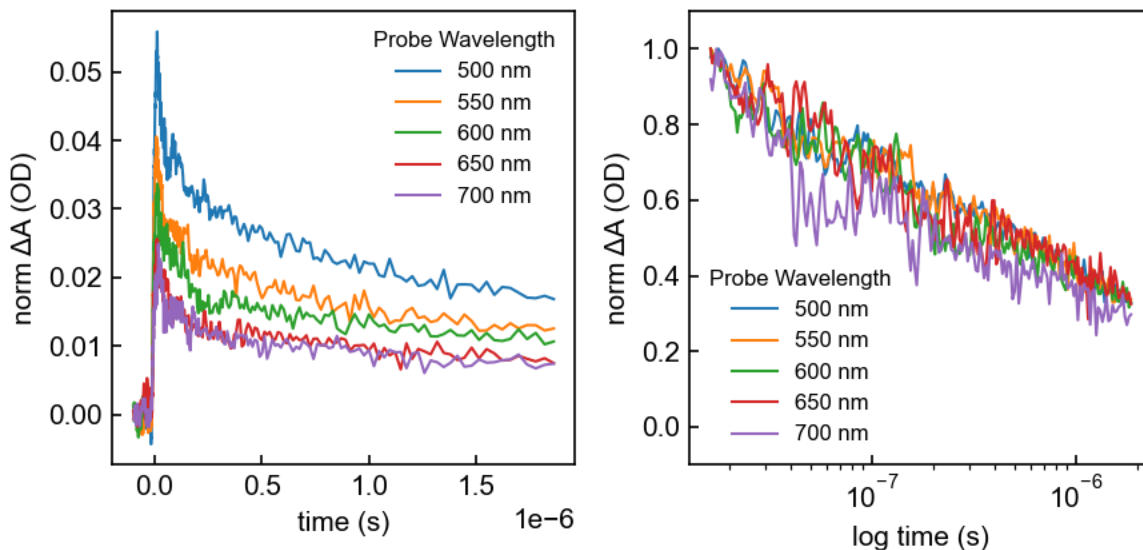


Figure S22. Decays of a CoPi film at various probe wavelengths, translating the film between scans to avoid dissolution effects and maintaining a constant detector gain for the transient absorption signal.

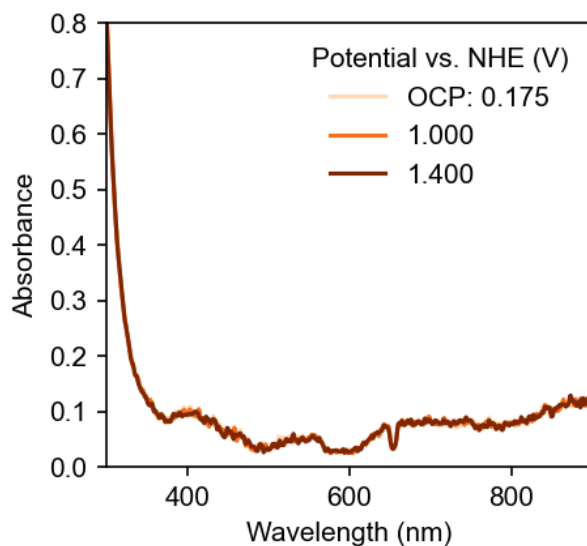


Figure S23: Unchanging spectral intensity with applied potential for an FTO film in phosphate buffer solution without the electrodeposited catalyst.

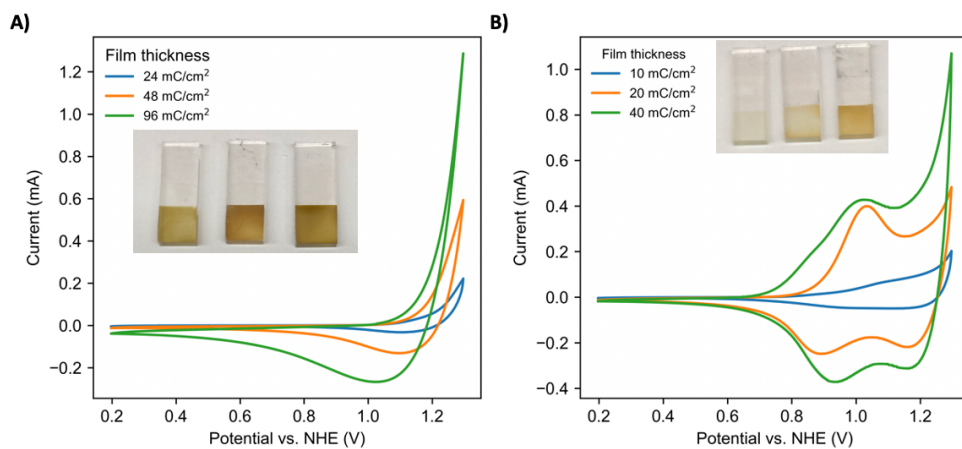


Figure S24: Cyclic voltammograms (first cycles) of 24, 48, and 96 mC/cm² CoPi (A) and 10, 20, 40 mC/cm² CoBi (B) films in their native buffers (pH 7.0 phosphate buffer for CoPi, pH 9.2 borate buffer for CoBi). Scan rates are 100 mV/s.

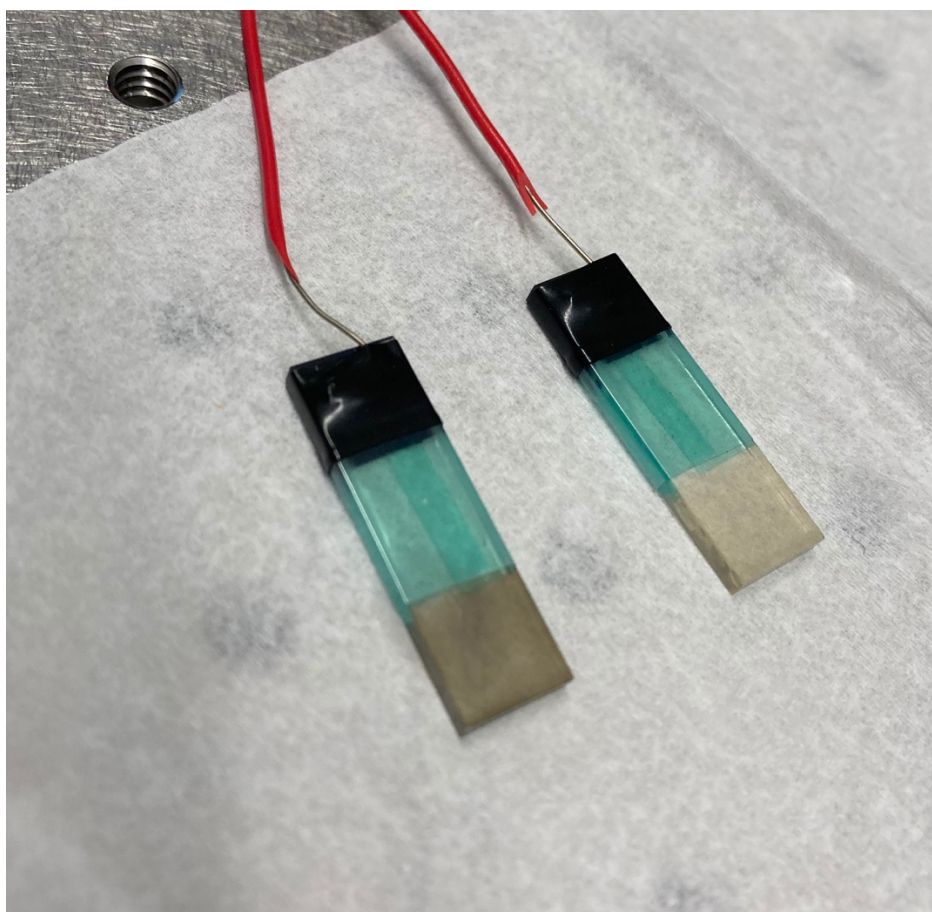


Figure S25. Pictures of two 10 mC/cm² CoPi films. On the left, the film has been under anodic bias for several hours. On the right, the film has only seen the anodic bias corresponding to the electrodeposition potential. The difference in visible absorption is apparent and quantified spectroelectrochemically.

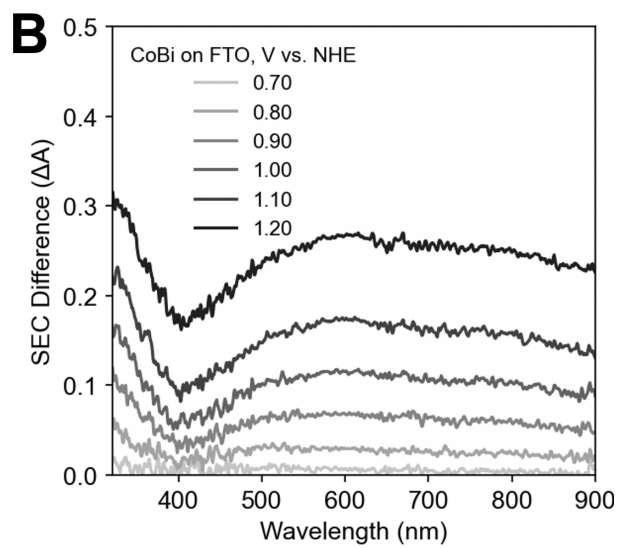
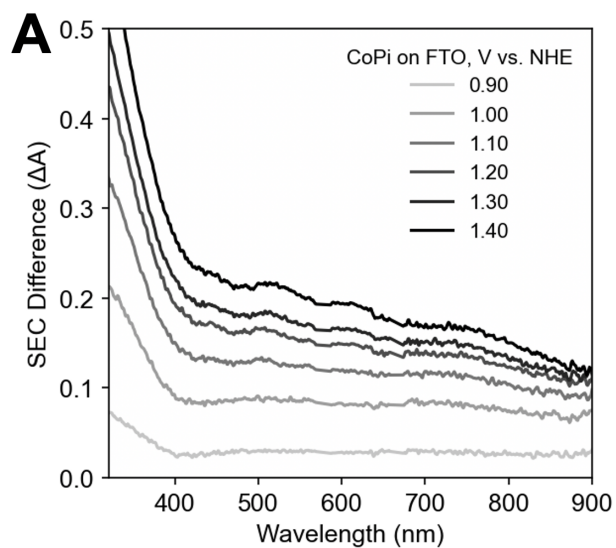


Figure S26. Spectroelectrochemical difference spectra (vs. NHE) of CoPi in pH 7.0 phosphate buffer (**A**) and CoBi in pH 9.2 borate buffer (**B**).

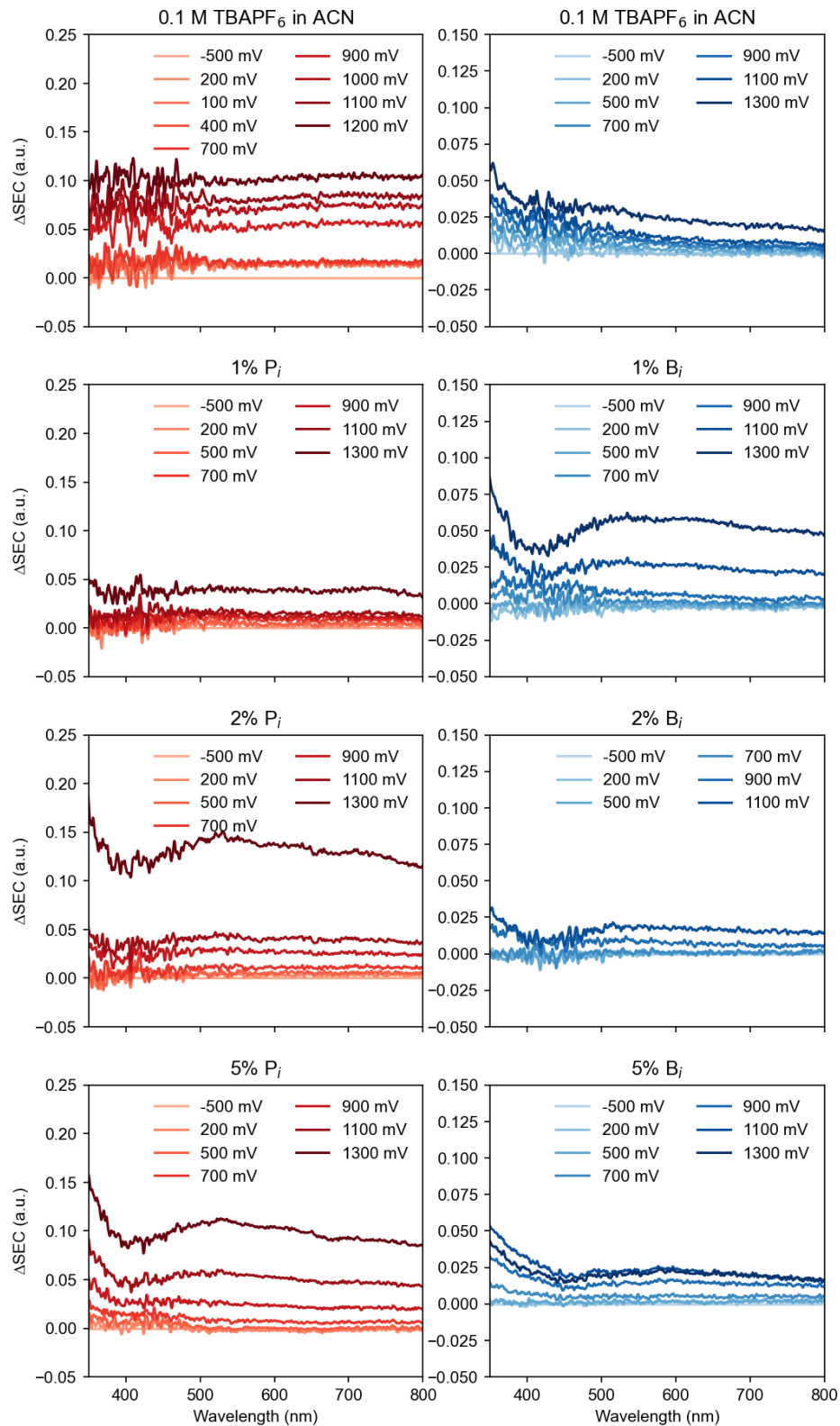


Figure S27. Spectroelectrochemical difference spectra (vs. 10 mM Ag/AgPF₆) of CoPi (left) and CoBi (right) in dry acetonitrile with 0.1 M TBAPF₆ with increasing amounts of aqueous buffer titrated in.

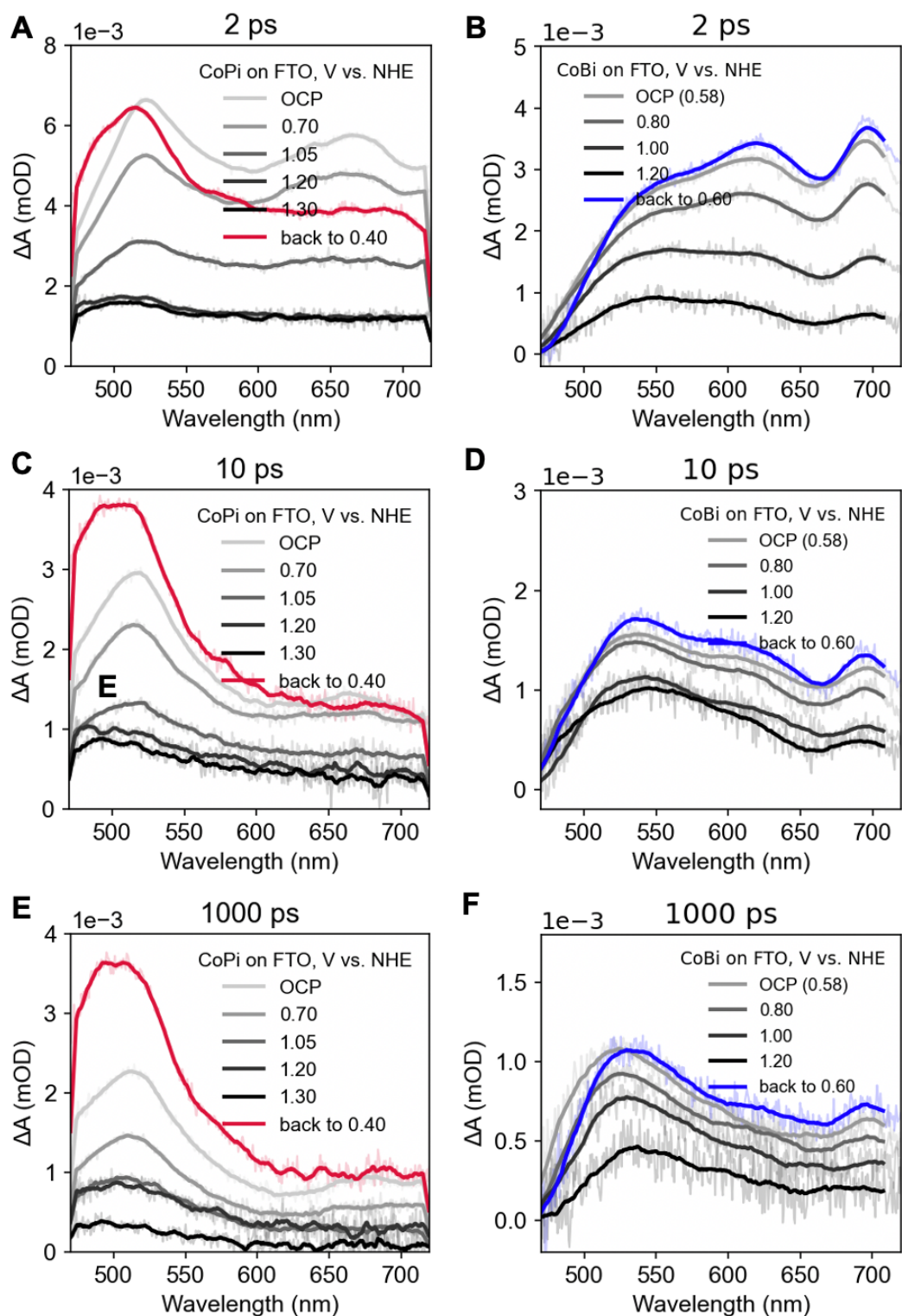


Figure S28. Transient absorption spectral traces at time delays of 2 ps, 10 ps and 1000 ps with applied bias of 96 mC/cm² CoPi (A, C, E) and 48 mC/cm² CoBi (B, D, F) films in their respective native buffers. Samples were pumped at 380 nm with a 120 fs pulse-width ultrafast laser.

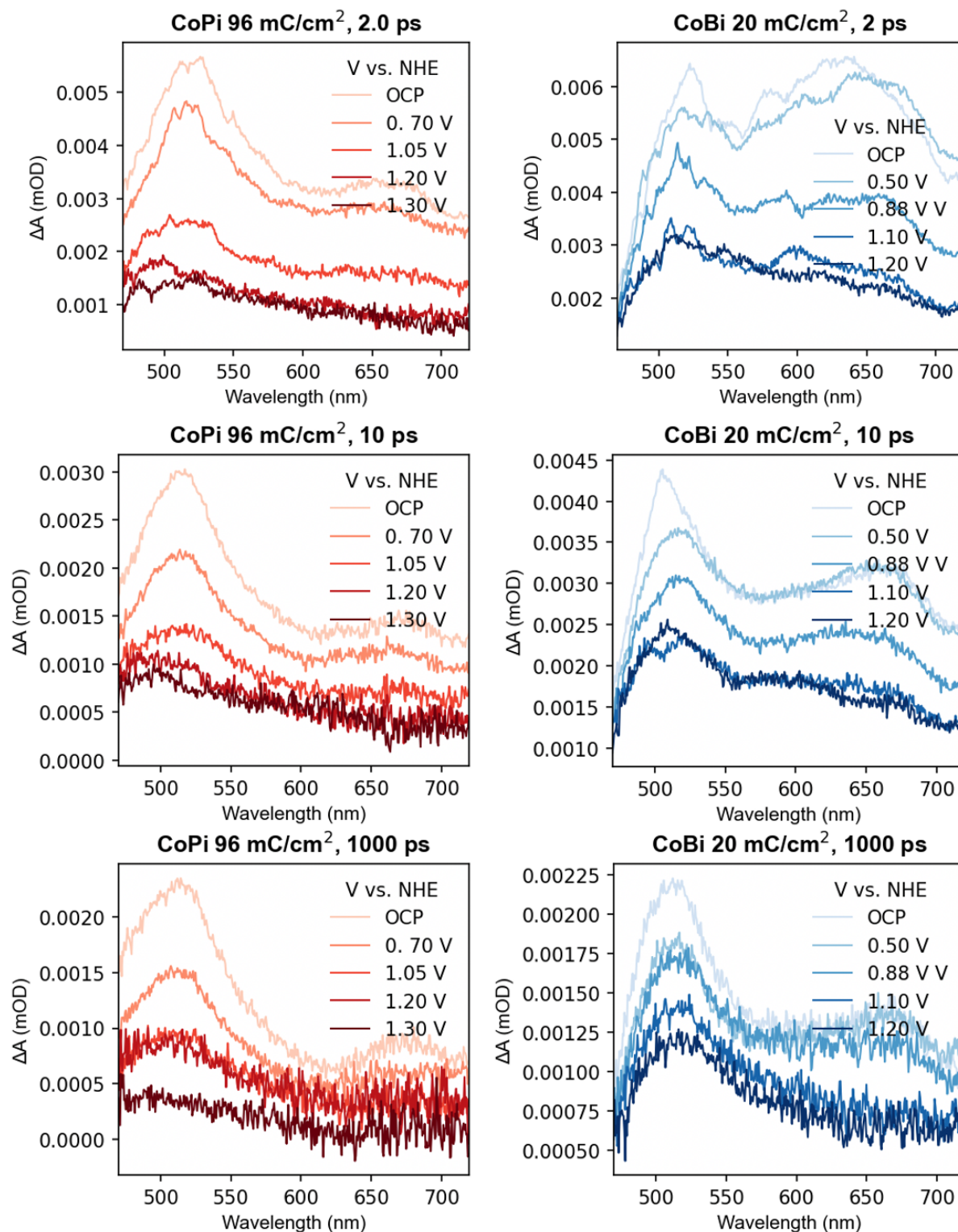


Figure S29. Transient absorption spectral traces at time delays of 2 ps, 10 ps and 1000 ps with applied bias of 96 mC/cm² CoPi and 20 mC/cm² CoBi films in their respective native buffers. Samples were pumped at 380 nm with a 120 fs pulse-width ultrafast laser.

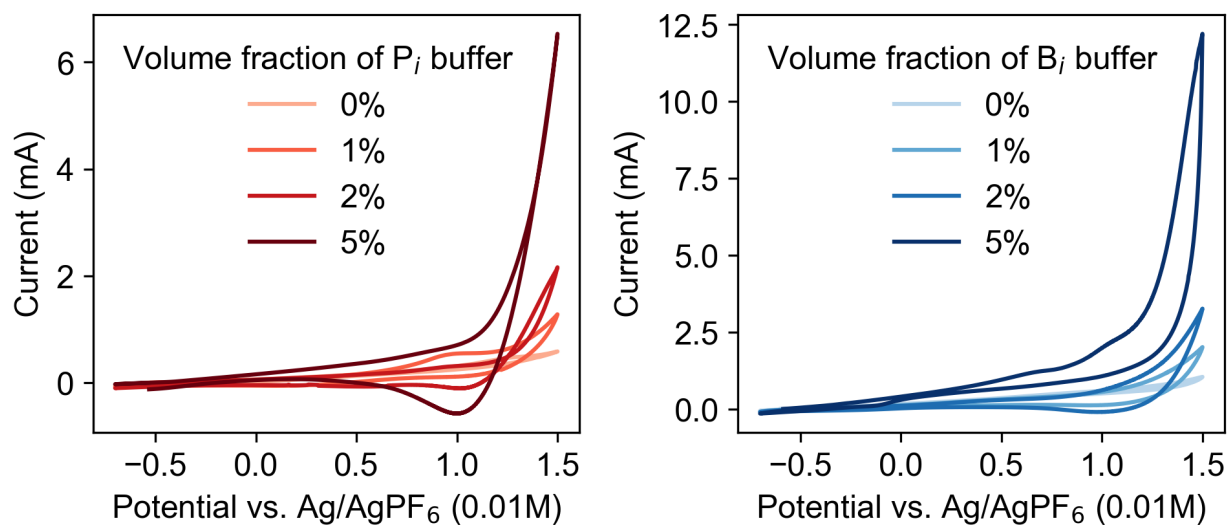


Figure S30. Cyclic voltammogram of CoPi (A) and CoBi (B) in dry acetonitrile with 0.1 M TBAPF₆ and corresponding amounts of respective aqueous buffer solutions added.

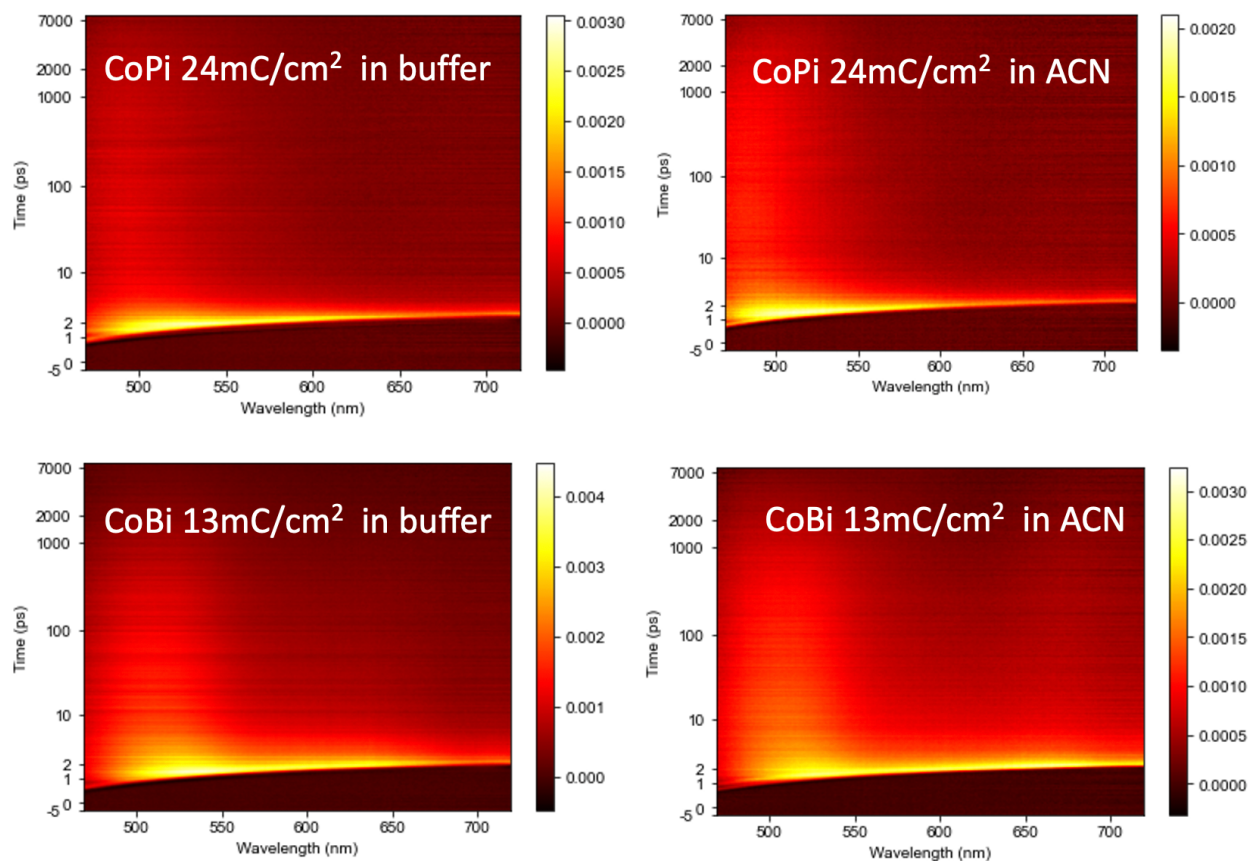


Figure S31. 2D transient absorption spectra of 24 mC/cm² CoPi and 13 mC/cm² CoBi films immersed in buffer and in acetonitrile.

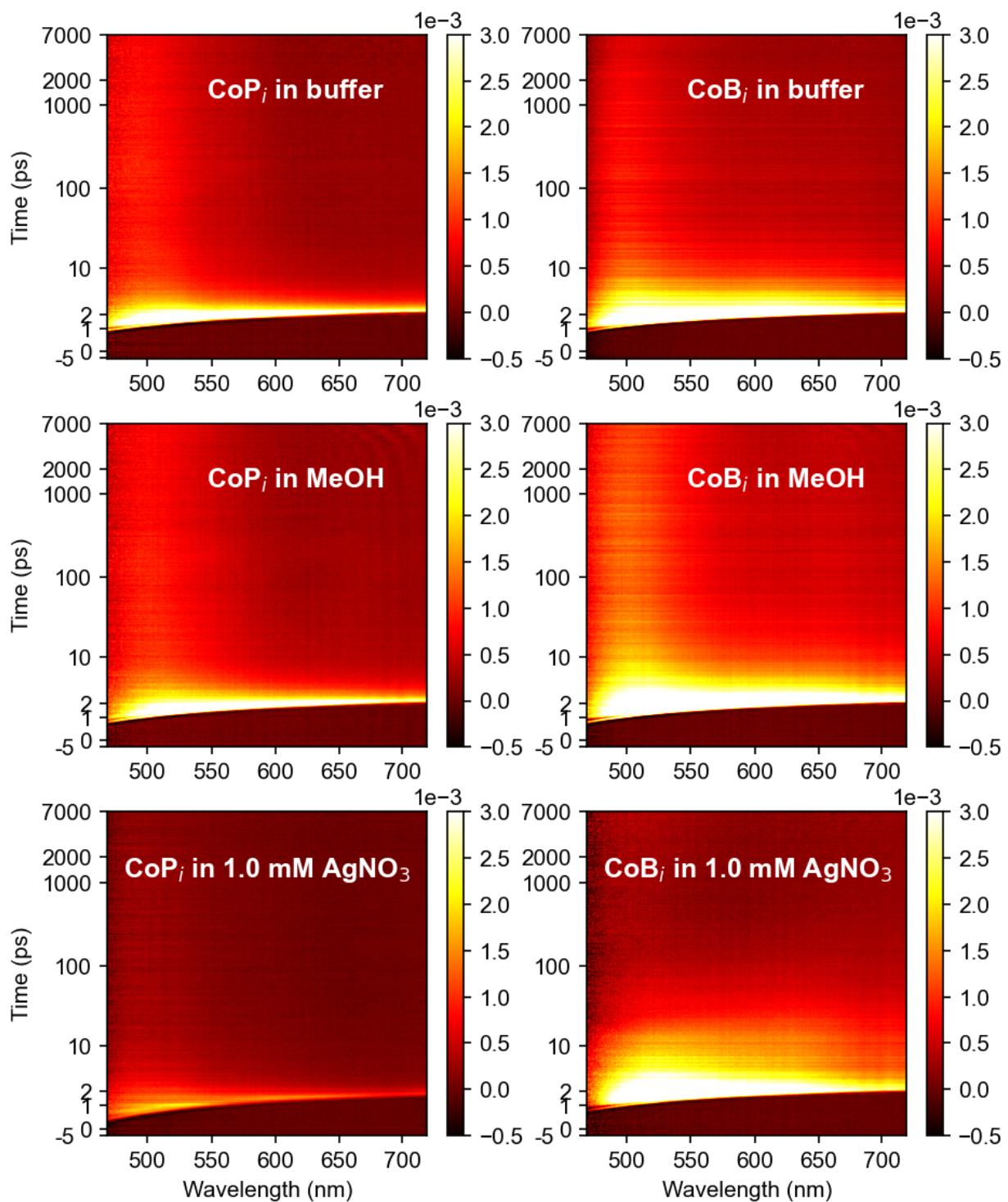


Figure S32. 2D transient absorption spectra of 48 mC/cm^2 CoPi and 20 mC/cm^2 CoBi films immersed in buffer, MeOH (hole scavenger) and aqueous AgNO_3 (electron scavenger) solutions.

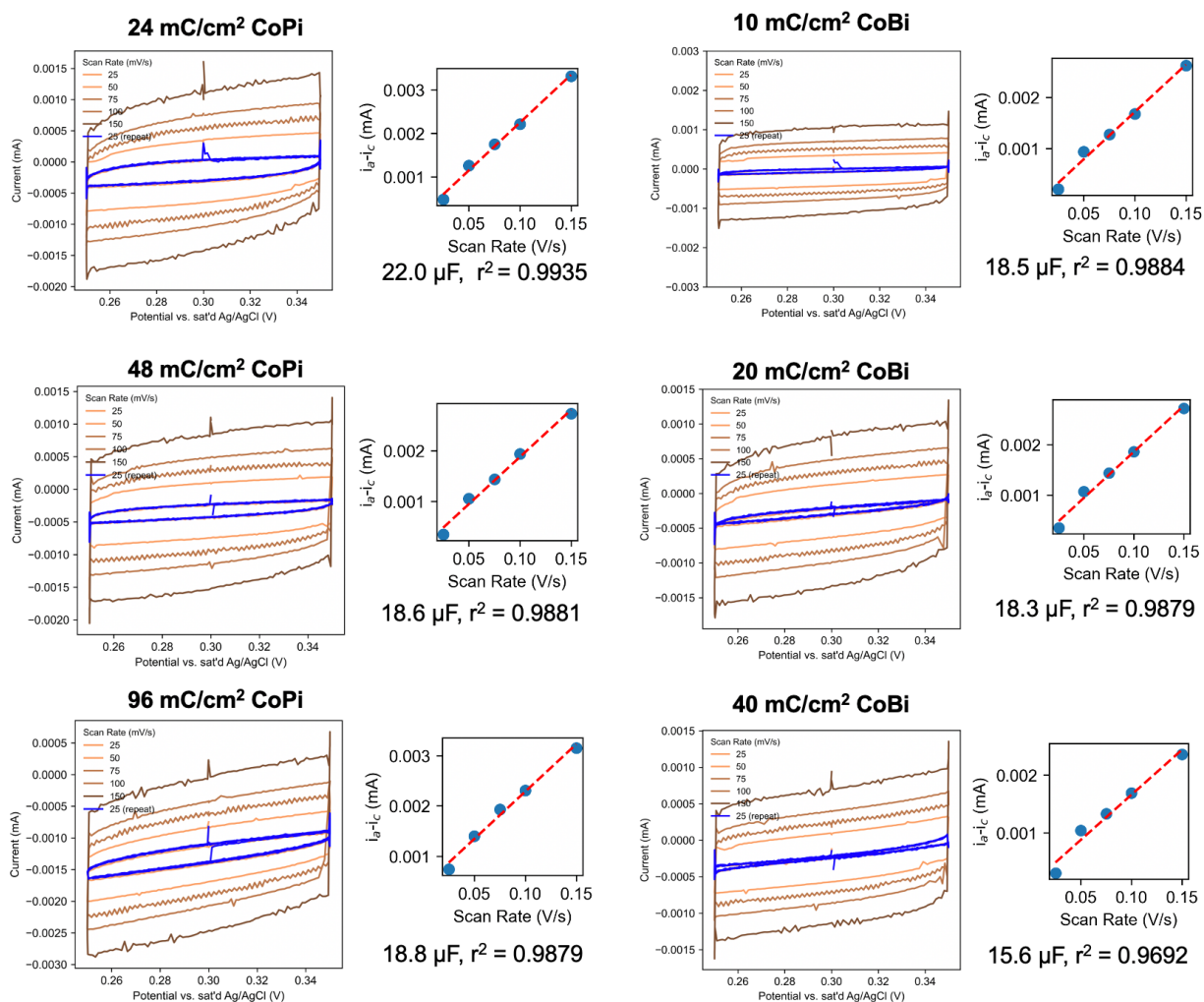


Figure S33: Scan rate dependence on non-faradaic regions of CVs of various film types and thicknesses in their native buffer solutions. The line of best fit yields a slope proportional to double layer capacitance, which is similar for the different film types and thicknesses. We note that the 75 mV/s scan rate data appears to have rapid oscillations in all cases due to an artefact with the data collection under the employed potentiostat settings. The “averaged” data are in line with the other measurements and therefore is still deemed reliable for this purpose.

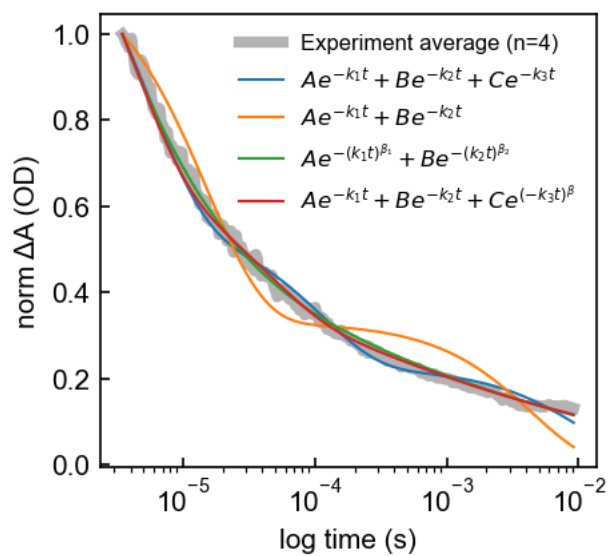


Figure S34. CoPi 10 ms time range average decay with various fitting models.

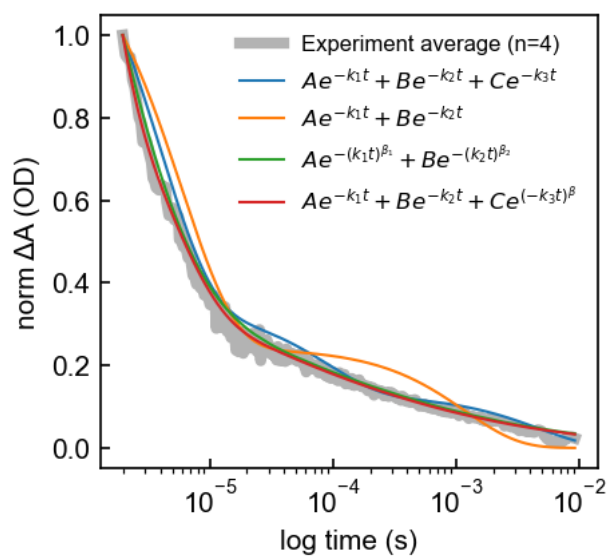


Figure S35. CoBi 10 ms time range average decay with various fitting models.

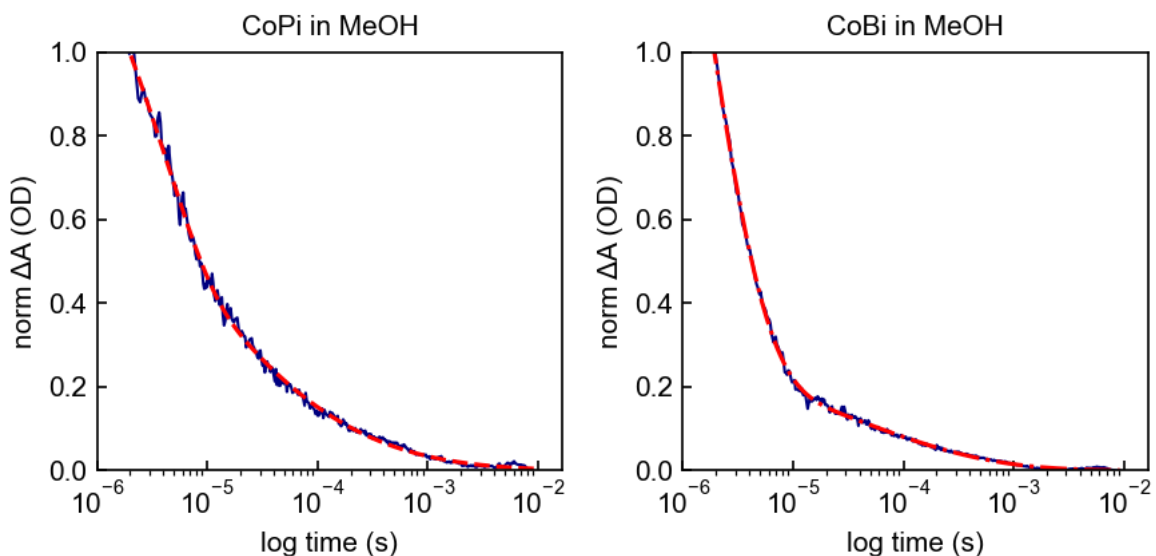


Figure S36. Normalized average 10 ms decays of CoPi ($n = 3$) and CoBi ($n = 2$) fit to two stretched exponentials. Details of fit given in Table S4.

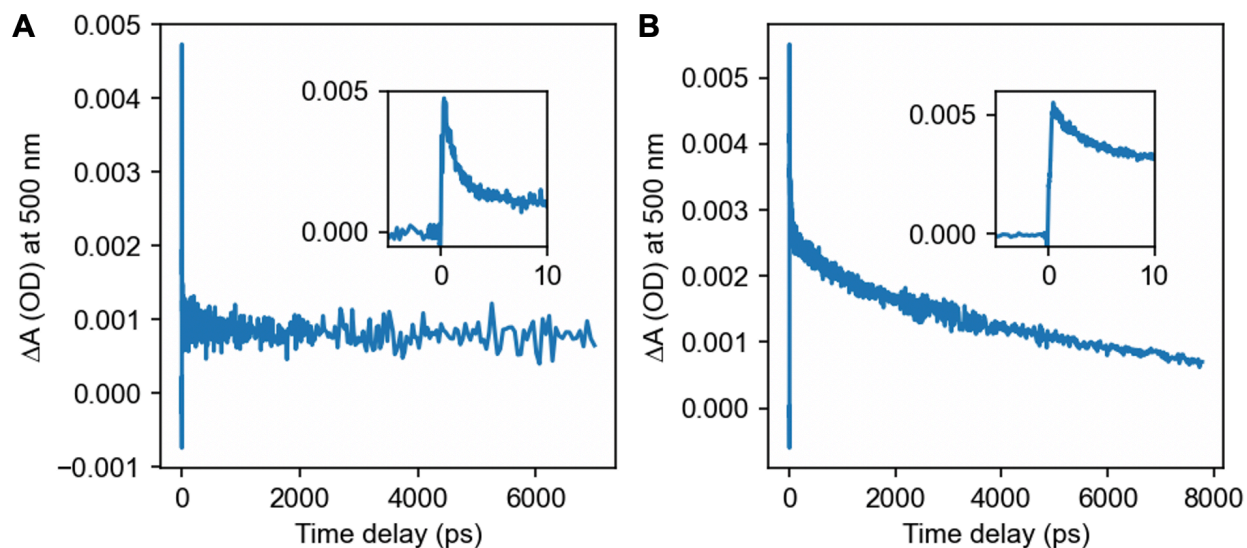


Figure S37. Ultrafast decay traces at 380 nm pump wavelength and 500 nm probe wavelength of 96 mC/cm^2 CoPi (A) and 40 mC/cm^2 CoBi (B). The insets show the decay before around time zero. The flat zero intensity line before time zero suggests that the 1 kHz repetition rate is appropriate for any measurable excited state population from the previous pump pulse to have decayed.

Tables

Table S1: Thickness data from profilometry.

Film	Charge passed (mC/cm ²)	Thickness via profilometry (nm)	Standard deviation (nm)
CoP _i	24	86	29 (n = 2)
CoP _i	48	473	73 (n = 2)
CoP _i	96	774	53 (n = 4)
CoB _i	10	108	10 (n = 4)
CoB _i	20	476	41 (n = 3)
CoB _i	40	1109	34 (n = 4)

Table S2: Fitting parameters for CoPi in H₂O: 10 ms time range kinetics.

	Triexponential
A	0.70
B	0.27
C	0.18
k ₁	184428
k ₂	8862
k ₃	91.0

	Two stretched exponentials
A	5.30

B	1.31
k ₁	1.96e+07
k ₂	6.06e+05
β ₁	0.233
β ₂	0.113

	Biexponential
A	0.66
B	0.26
k ₁	65440
k ₂	226.5

	Two exponentials, one stretched exponential
A	0.14
B	0.58
C	1.61
k ₁	21440
k ₂	256400
k ₃	3.83e+06
β	0.099

Table S3: Fitting parameters for CoBi in H₂O: 10 ms time range kinetics

	Triexponential
A	0.98
B	0.19
C	0.11
k ₁	260675
k ₂	11164
k ₃	213.7

	Two stretched exponentials
A	3.19
B	1.30
k ₁	1.70e+06
k ₂	1.91e+06
β ₁	0.468
β ₂	0.134

	Biexponential
A	0.88
B	0.20
k ₁	169553
k ₂	841

	Two exponentials, one stretched exponential
A	0.61
B	3.01
C	1.68
k ₁	226045
k ₂	1.46e+06
k ₃	7.73e+06
β	0.123

Table S4: Fits of two stretched exponentials to the normalized average decay of CoPi in MeOH and CoBi in MeOH.

	CoPi
A	0.40
B	3.87
k ₁	2.00e+05
k ₂	1.25e+07
β ₁	1.20
β ₂	0.16

	CoBi
A	2.76
B	0.36
k ₁	7.39e+05

k_2	3.48e+04
β_1	0.72
β_2	0.33

References

- (1) Kanan, M. W.; Nocera, D. G. In Situ Formation of an Oxygen-Evolving Catalyst in Neutral Water Containing Phosphate and Co^{2+} . *Science* **2008**, *321* (5892), 1072–1075. <https://doi.org/10.1126/science.1162018>.
- (2) Surendranath, Y.; Kanan, M. W.; Nocera, D. G. Mechanistic Studies of the Oxygen Evolution Reaction by a Cobalt-Phosphate Catalyst at Neutral pH. *J. Am. Chem. Soc.* **2010**, *132* (46), 16501–16509. <https://doi.org/10.1021/ja106102b>.
- (3) Brodsky, C. N.; Bediako, D. K.; Shi, C.; Keane, T. P.; Costentin, C.; Billinge, S. J. L.; Nocera, D. G. Proton–Electron Conductivity in Thin Films of a Cobalt–Oxygen Evolving Catalyst. *ACS Appl. Energy Mater.* **2019**, *2* (1), 3–12. <https://doi.org/10.1021/acsaem.8b00785>.
- (4) McCrory, C. C. L.; Jung, S.; Ferrer, I. M.; Chatman, S. M.; Peters, J. C.; Jaramillo, T. F. Benchmarking Hydrogen Evolving Reaction and Oxygen Evolving Reaction Electrocatalysts for Solar Water Splitting Devices. *J. Am. Chem. Soc.* **2015**, *137* (13), 4347–4357. <https://doi.org/10.1021/ja510442p>.
- (5) Bruker Corporation. *DektakXT Stylus Profiler User Manual*; Bruker Corporation, 2011.